INFORMATION TO USERS

This manuscript has been reproduced from the microfilm master. UMI films the text directly from the original or copy submitted. Thus, some thesis and dissertation copies are in typewriter face, while others may be from any type of computer printer.

The quality of this reproduction is dependent upon the quality of the copy submitted. Broken or indistinct print, colored or poor quality illustrations and photographs, print bleedthrough, substandard margins, and improper alignment can adversely affect reproduction.

In the unlikely event that the author did not send UMI a complete manuscript and there are missing pages, these will be noted. Also, if unauthorized copyright material had to be removed, a note will indicate the deletion.

Oversize materials (e.g., maps, drawings, charts) are reproduced by sectioning the original, beginning at the upper left-hand corner and continuing from left to right in equal sections with small overlaps.

ProQuest Information and Learning
300 North Zeeb Road, Ann Arbor, MI 48106-1346 USA
800-521-0600

University of Alberta

Role of Fine Solids in Coke Formation during Residue Conversion

by

Weidong Bi 

A thesis submitted to the Faculty of Graduate Studies and Research in partial fulfillment

of the requirements for the degree of Master of Science

in

Chemical Engineering

Department of Chemical and Materials Engineering

Edmonton, Alberta

Fall 2005

To Yingchun

Abstract

Hydrophobic fine solids can reduce the yield of toluene-insoluble (TI) coke in thermal cracking of heavy oils at short reaction times. In this work, two carbonaceous fine solids were used as additives in coking of Arab Heavy Vacuum Residue (AHVR) in 1-methylnaphthalene (1-MN) to study the mechanism of this interaction.

Both fine additives significantly reduced the coke yield compared with the case of no solid addition. Coke deposited on the surfaces of the two hydrophobic additives. This nucleation of coke deposition on the solid reduced the agglomeration of the coke, giving a better dispersion in the liquid. The highly dispersed coke phase on fine solids was more accessible for reactions with hydrogen donor compounds in the oil phase, which in turn inhibited the initial rate of coke formation.

Acknowledgements

I would like to express my sincere thanks to those who assist me in achieving my goal today, although some of their names may be absent here.

I am full of gratitude to my supervisor, Dr. Murray Gray, for his thoughtful guidance and support throughout my program. His advice, inspiration and encouragement are crucial to the completion of this thesis. I would also like to thank my cosupervisor, Dr. William McCaffrey, whose valuable suggestions are beneficial to my project.

Many others have also contributed to the work in this thesis. I am grateful to Ms. Tina Barker and Mr. George Braybrook for helping me in SEM and EDX analyses. I thank Dr. Dimitre Karpuzov and Dr. Anqiang He for their help in XPS analysis. I appreciate Mr. Jim Skwarok for teaching me to use the Mastersizer for particle size measurement.

My colleges in the Heavy Oil Upgrading Research Group have been a great help on a daily basis, in particular, Ms. Tuyet Le, Mr. Oswaldo Asprino, Mr. Pedro Gonzales, Mr. Jeff Sherimatta. I would also like to thank people in the Department of Chemical and Materials Engineering for their assistance throughout my research here, especially Ms. Andree Koenig and Mr. Walter Boddez.

My eternal gratitude goes out to my dear wife, Ms. Yingchun Zhao, for her unselfish sacrifice to the family, and for all the experience we shared during the tough time. This appreciation should undoubtedly be extended to my parents for their love and spiritual support despite the long distance between us. I cannot forget to say sorry to my adorable daughter, Francie, for the time I should have been around her.

Table of Contents

List of Tables

List of Figures

1. INTRODUCTION

1.1 BACKGROUND

Petroleum and fossil fuels are non-renewable resources. As the world's supply of conventional crude oil declines, heavy oil and bitumen are becoming more and more important feeds to meet the world's growing demands for fuels and petrochemicals. World heavy oil and bitumen resources exceed the resources of conventional oils and will become the principle source of crude oils in the early 21st century (Strausz and Lown, 2003).

Oil sands are a major source for bitumen. Canada has the world's largest known oil sands deposit, which is found mainly in three areas of Alberta – Athabasca, Cold Lake and Peace River. A typical sample of oil sands might contain about 12 percent bitumen by weight (Petroleum Communication Foundation, 2000). The 1.6 trillion barrels of bitumen in Canada's oil sands are the world's largest single hydrocarbon resource, of which over 300 billion barrels are recoverable by current technologies. Bitumen, however, contains as much as 50 wt% of non-distillable residues and must be upgraded or diluted before it will flow into a refinery through a pipeline. Residues are of little market value, and usually are upgraded to lighter, more valuable oil products in refineries.

The goal of upgrading bitumen and residues is to convert high boiling and low H/C ratio feeds into lower boiling and higher H/C ratio distillates and remove the heteroatoms such as sulfur and nitrogen down to environmentally acceptable levels. To turn this goal into reality, the hydrocarbon molecules need to undergo a number of thermal and

catalytic reactions during the upgrading processes. According to the approaches to achieve higher H/C ratios, the upgrading processes can be classified into two categories: those with carbon rejection and those with hydrogen addition. The carbon rejection processes achieve higher H/C ratios by rejecting a percentage of carbon from the feed. Industrial processes using this approach include coking such as delayed coking and fluid coking, catalytic cracking such as the FCC (Fluid Catalytic Cracking) process, and solvent deasphalting such as the ROSE (Residuum Oil Supercritical Extraction) process (Speight and Özüm, 2002). In contrast, the hydrogen addition processes increase H/C ratio by adding hydrogen atoms to hydrocarbon molecules. Commercial hydrogen addition processes include ebullated bed technologies such as LC-Fining and H-Oil processes, and slurry bed technologies such as the VCC (VEBA-COMBI-Cracking) process and the CANMET hydroconversion process. Hydrogen addition processes usually give higher quality and higher yield of the desirable products. However, these processes require participation of both hydrogen and catalysts, which results in higher capital and operating costs compared with the carbon rejection processes.

As one of the oldest technologies available for residue conversion, coking processes do not require addition of catalyst and are very efficient in rejecting mineral solids and metals along with some organic nitrogen and sulfur in the coke, though the efficiency of rejection of sulfur into coke is low. Coking is a thermal process where the feed is cracked to produce gases, distillates and coke. Today in Canada, coking processes such as delayed coking and fluid coking, are playing an important role in processing bitumen and heavy oil. For example, as a primary upgrading process, coking is the most commonly employed technology to upgrade bitumen into synthetic crude oil.

In both delayed coking and fluid coking processes, the formation of gases and distillates which have higher H/C ratio compared with the feed, inevitably leads to the formation of a by-product called coke, a solid carbonaceous material that has a much lower H/C ratio. Although the formation of coke in hydrogen addition processes is reduced due to the presence of hydrogen, its impact on process operation is not negligible. Coke formation causes deactivation of catalysts and shortens the run length of units, and thus has to be minimized (Butt and Petersen, 1988). In addition, coke deposits that accumulate in process equipment are responsible for the fouling of furnace tubes, heat exchangers, reactors and separators (Watkinson and Wilson, 1997; Lemke and Stephenson, 1998). Although coke is accepted as a by-product in coking processes, excessive coke formation is economically undesirable because coke is of much lower value than distillates. Syncrude Canada, the operator of the world's largest fluid cokers to process oil sands bitumen, has been stockpiling the coke due to the lack of market demand. Therefore, in order to maximize the yield of much valuable distillates, coke formation has to be controlled.

Athabasca bitumen recovered by the combination of surface mining and hot water extraction technologies contains a high content of fine solids known as bitumen solids. Bitumen solids cause many operational problems such as plugging of hydrotreaters and fouling of process vessels. One study (Tanabe and Gray, 1997) has found that bitumen solids, despite their negative impact on process operation, have a remarkable influence on the initial kinetics of coke formation under coking conditions, which seems favorable to help control the undesirable by-product of coke. Relevant studies have also discovered a similar trend by adding additional fine solids (Sanaie et al., 2001; Liu, 2002). The

mechanism of the effect of fine solids on kinetics of coke formation, however, has not been well defined. Further study on this mechanism is required to determine if this mechanism can be used to enhance coking processes or to suppress unwanted coke deposition in process equipment.

1.2 RESEARCH OBJECTIVES

Previous studies had found that the presence of fine solids had a significant impact on the initial kinetics of coking. Hydrophobic fine solids reduced coke yield significantly at short reaction times. The major objectives of this work are to answer two research questions:

(1) What is the physical interaction between fine solids and the coke phase in coking?

Some studies have pointed out that fine solids disperse the liquid coke phase as it forms, reducing its tendency to coalesce into large domains. Direct evidence of interaction between solids and coke phase, however, is lacking. In this work, two novel carbon materials were used as a hydrophobic base for depositing coke, in order to study the formation of coke in a controlled geometry in liquid suspension. Different analytical methods were employed to investigate the morphology of solid particles.

(2) What is the chemical mechanism of reducing coke yields due to fine solids?

The presence of hydrophobic fine solids retards coke formation at short reaction times under coking conditions, as confirmed by several studies, but the mechanism involved in this reaction process is still under argument. Based on the direct evidence of the interaction between solids and coke phase obtained in this work, the mechanism was further investigated through specialized experimental design.

2. -LITERATURE REVIEW

2.1 BITUMEN AND VACUUM RESIDUE

Bitumen and vacuum residue are generally defined in terms of their physical properties. A typical dictionary definition of bitumen is "a tar-like mixture of petroleum hydrocarbons." In the oil-producing industry, bitumen is more technically defined as petroleum having a viscosity grater than 10^4 mPa·s and a density grater than 1.0 g·cm^{-3}, corresponding to an API gravity of less than 10 degrees, as shown in Table 2.1. Vacuum residue is operationally defined as the fraction that does not distill under vacuum, with atmospheric equivalent boiling points over 524 °C. In a refinery this fraction would be produced as the bottom product from a vacuum distillation column (Sanford 1991).

Table 2.1 Classification of crude oils according to grade (Strausz and Lown, 2003)

Grade of oil	Specific gravity, g·cm^{-3} at 15.6 °C	API gravity	Viscosity, mPa·s
Conventional light oil	< 0.876	> 30	
Conventional medium oil	0.876-0.934	20-30	
Heavy oil	0.934-1.00	10-20	$\leq 10^3$
Extra heavy oil	> 1.00	< 10	$\leq 10^4$
Bitumen	> 1.00	< 10	$> 10^4$

The properties of bitumen and residues depend on their chemical composition.

Bitumen and residues are very complex mixtures containing thousands or even millions of different molecules without a repeating molecular unit (Zander, 1987; Wiehe and Liang, 1996), which makes component-by-component analysis extremely difficult.

The SARA (saturate-aromatic-resin-asphaltene) method, originally designed for characterization of residual oils (Jewell et al., 1974), is a widely used separation scheme based on combined solubility and adsorption characteristics of bitumen or residue. By using the experimental SARA procedure, the heavy end of a crude oil can be separated into four distinct fractions namely saturates, aromatics, resins, and asphaltenes. This separation sequence is illustrated in Figure 2.1. Asphaltenes are the class of compounds that are soluble in an aromatic solvent such as toluene or benzene but insoluble in *n*-alkanes such as *n*-heptane or *n*-pentane. The yield and quality of this fraction depends on how it is separated, the ratio of the solvent to oil, the time before filtration, the pore size and material of the filter etc. However, by keeping these variables constant, a reproducible yield and quality can be obtained. The n-alkane soluble fraction is defined as maltenes. Maltenes can further be separated by adsorption column chromatography. Usually silica gel or alumina is used as the adsorbent, and the separation is carried out by elution with different solvents. Maltenes can thus be separated into three fractions (Speight, 1994): 1) saturates, eluted with n-heptane, 2) aromatics, eluted with benzene, and 3) resins, eluted with benzene/methanol. Besides these four fractions, a toluene-insoluble fraction may be present in some bitumens such as the Athabasca bitumen, which is commonly classified as bitumen solids. Considering the difference between solubility classes separated using

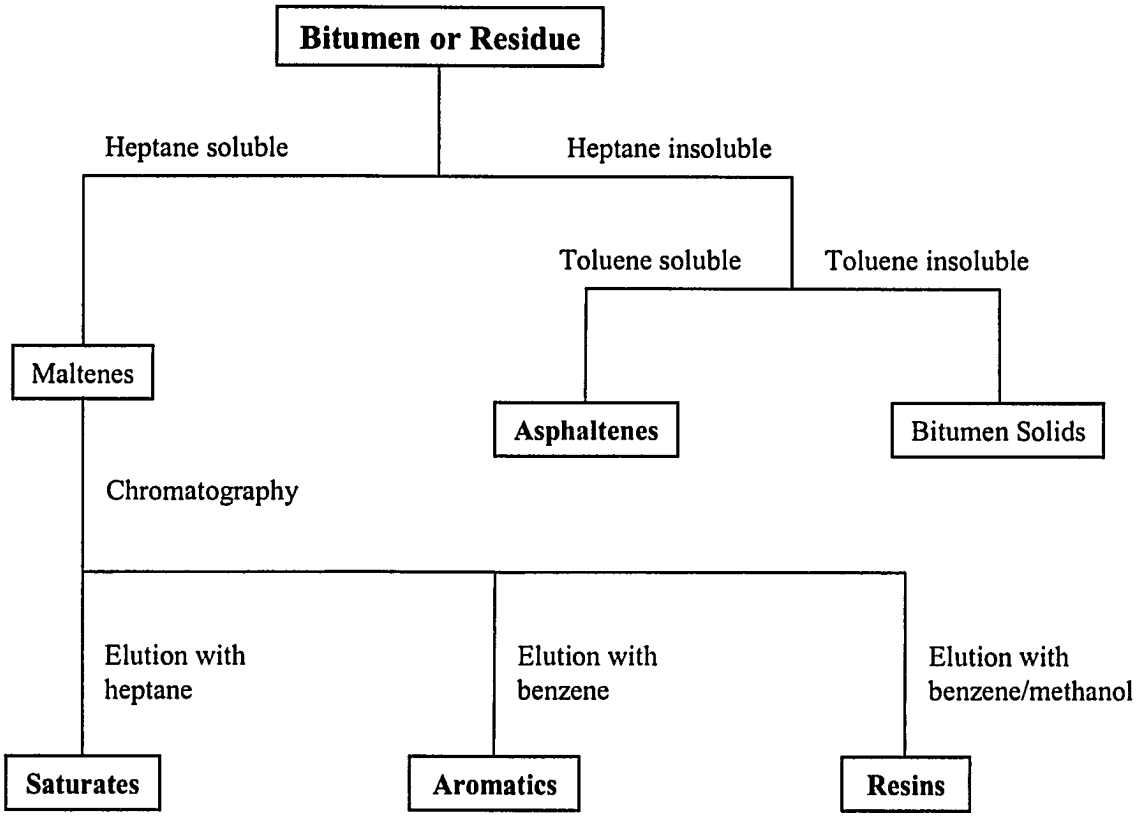

Figure 2.1 Schematic of bitumen or residue separation into solubility classes.

different methods, it is important to explicitly specify the separation solvents when referring to those solubility classes, for example, heptane-insoluble asphaltenes or pentane-insoluble asphaltenes.

In spite of the apparent homogeneity, bitumen and vacuum residue are not true solutions, but colloidal dispersion systems of the asphaltenes in the other fractions (Pfeiffer and Saal, 1940; Koots and Speight, 1975; Storm et al., 1991; Bardon et al., 1996; Speight and Long, 1996; Loeber, 1998; Li et al., 1999). The resin fraction has often been described as an asphaltene stabilizer. At ambient temperatures, asphaltenes are dispersed by the surfactant-like resins. Without the resin fraction, asphaltenes are generally non-dispersible in the remaining oil. Some measurements (Kumagai, 2003; Tanaka et al. 2004) support that aggregation of asphaltenes decreases as temperature increases, whereas an opposite view (Storm et al., 1996) suggests that asphaltenes can flocculate due to disruption of the dispersing resins well below the temperature at which chemical reactions occur.

2.2 ASPHALTENES

Petroleum asphaltenes are defined as organic material soluble in toluene and insoluble in *n*-heptane or *n*-pentane. Asphaltenes are such complex mixtures that it is impossible to obtain an exact molecular description using current analytical techniques. Some information about the chemical and physical structures, however, can be elucidated by some methods, such as FTIR (Lian et al., 1994), ^{13}C and H-NMR (Storm et al., 1994), and small-angle X-ray scattering (Herzog et al., 1988; Storm et al., 1993). Petroleum

asphaltenes are widely reported to be condensed aromatic systems carrying aliphatic and naphthenic chains, various functional groups, and heteroatom substituents.

There are appreciable amounts of organic non-hydrocarbon constituents present in asphaltenes, mainly sulfur, nitrogen and oxygen and, in smaller amounts, organo-metallic compounds (Speight, 1991). Sulfur compounds are found mainly in two forms, in aromatic rings, which are very stable, and in thio-ethers or organic sulfides, which have weaker bonds and are more easily thermally cracked. Nitrogen compounds are also found mainly in two forms, one composed mainly of pyridine homologs, and the other of pyrrole, indole and carbazole types. Both types of nitrogen compounds are highly resistant to removal. Oxygen may be present in aromatic rings, bonded directly to carbon ethers, and as other polar functional groups such as hydroxyls and acids. Trace amounts of metals, mostly vanadium and nickel, are found in two organic forms in asphaltenes: porphyrin metals, which are chelated in porphyrin structures, and non-porphyrin metals, which are thought to be associated with the polar groups of asphaltenes (Gray, 1994).

Yen and coworkers (Yen et al., 1961; Dickie and Yen, 1967) showed the crystal-like microstructure of asphaltenes using X-ray diffraction. They proposed that asphaltenes are aggregates of polycyclic aromatic sheets. Each sheet is formed by bonding of the aromatic cores of about four to five asphaltenic molecules and then the sheets form aggregates by hydrogen bonding or other dipole-dipole interactions. The size of the aromatic groups and the molecular weight of asphaltenes has been a matter of considerable controversy for some years. Different methods, including vapor pressure osmometry (VPO), gel

permeation chromatography (GPC), mass spectrometry (MS) and fluorescence depolarization, have been used to determine the molecular weight of asphaltenes (Strausz et al., 2002; Groenzin and Mullins, 2000). Asphaltenes have a high tendency for self-association, which has made the apparent molecular weight vary considerably from around 500 to as high as 100,000 depending on the technique and conditions employed for the measurements (Moschopedis et al., 1976). For instance, the molecular weight of asphaltenes from Athabasca bitumen has been reported having a range from 885 to 10,910 (Champagne et al., 1985). The high values are not the true molecular weight of the asphaltenes, but the average "molecular weight" of aggregates of the self-associated asphaltenes. For the method of VPO, more reliable and consistent average molecular weight of asphaltenes could be reached in highly dissociating solvents such as nitrobenzene, pyridine and o-dichlorobenzene at the highest feasible temperatures and the lowest feasible concentrations (Speight et al. 1985; Wiehe, 1992).

Despite the chemical complexity and diversity of asphaltenes, some efforts have been made to construct the molecular structure of asphaltenes. Strausz and co-workers (Strausz et al., 1992; Murgich et al., 1999) proposed hypothetical asphaltene structures based on the chemical and thermal decomposition studies of acetone-extracted asphaltene from Athabasca bitumen. Their study suggested that the extent of aromatic condensation is low and that highly condensed pericyclic aromatic structures are present in very low concentrations. Sheremata et al. (2004) created a series of molecular representations to quantitatively describe the Athabasca asphaltenes. According to their study, at least five

representative molecules are needed to accurately fit the analytical data from elemental analysis, molecular weight by VPO and both ^{1}H and ^{13}C-NMR spectroscopy. Their study provided the first quantitative molecular representation of asphaltenes as archipelago structures, with all of the generated structures composing of islands of relatively small aromatic clusters that connected together by aliphatic and sulfur side chains. Figure 2.2 shows a molecular representation of the Athabasca asphaltenes by their study.

Asphaltenes play a central, often a hindering role in the utilization of hydrocarbon resources. The increased asphaltene content is mostly responsible for the increase in viscosity, which may cause serious difficulties in the production and transportation of crude oil. From the upgrading point of view, asphaltenes are believed to be the major contributor to coke formation, which in turn may cause some operational problems such as plugging and fouling.

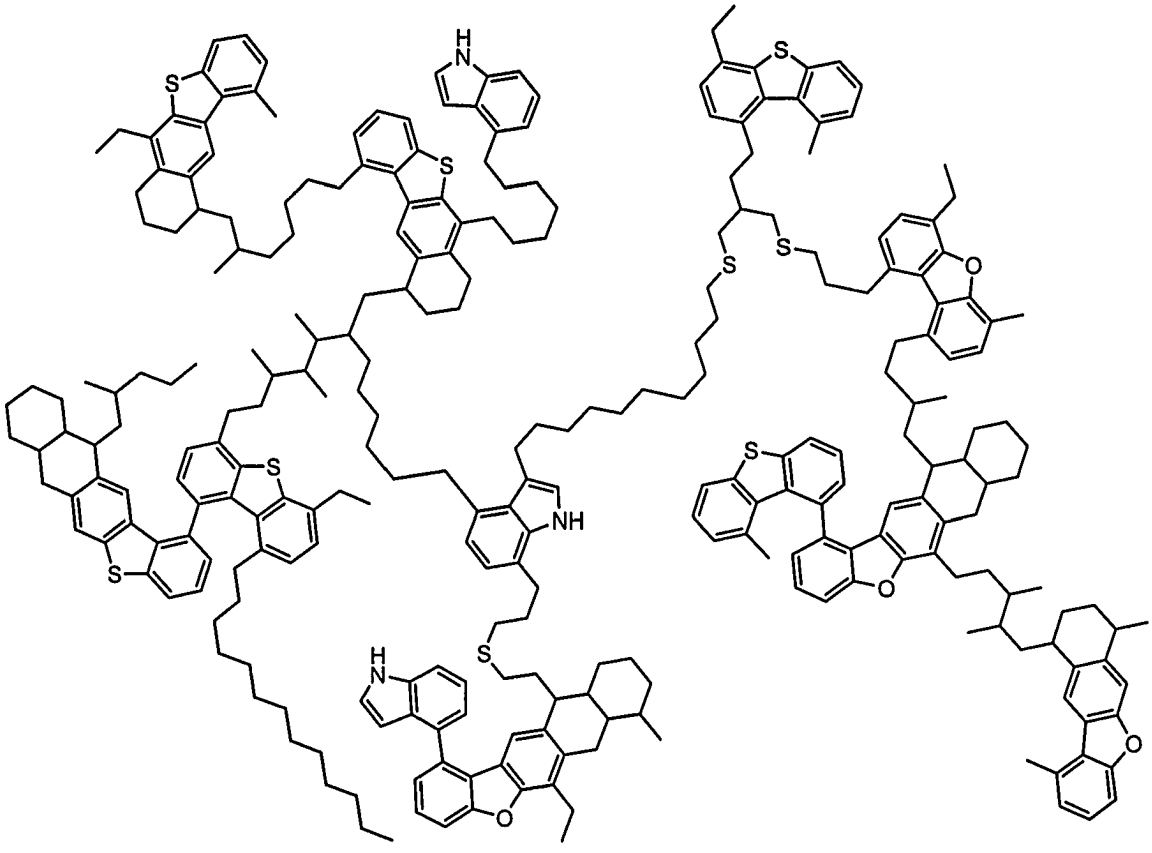

Figure 2.2 Molecular representation of Athabasca asphaltenes

(Sheremata et al., 2004).

Chemical Formula: $C_{283}H_{337}N_3O_4S_9$; Molecular Weight: 4133 g/mol

2.3 THERMAL CRACKING REACTIONS

The various upgrading processes for bitumen and residues conversion share common reaction chemistry and thermodynamics. The commercial processes for production of distillate products from vacuum residues operate at 410-555 °C where thermal cracking reactions are significant. In cracking reactions, the big hydrocarbon molecules in bitumen and residues are decomposed into small ones by bond breakage. Thermal cracking reactions of heavy hydrocarbon mixtures occur spontaneously at significant rates at temperatures higher than 400 °C (Poutsma, 1990; Gray, 1994). Catalytic cracking is not significant unless the residue has low contaminant level so that it can be blended into fluid catalytic cracking or hydrocracking with a gas oil feed.

The cleavage of carbon-carbon bonds is achieved mainly via free radical chain reactions. Free radical pathways dominate mechanisms for thermal cracking of organic materials (Poutsma, 2000). Free radicals are neutral species with unpaired electrons, highly energetic, short lived and present at very low concentrations. The relative degree of difficulty in breaking a particular bond to form free radicals can be partially described by the bond dissociation energies. The dissociation energies of some common bonds are listed in Table 2-2. The main bonds of interest during primary upgrading are C-C, C-H and C-S bonds. The C-S bonds are considerably weaker than C-C bonds and C-H bonds and hence are the first to break. The C-C bonds in aromatic hydrocarbons are much stronger due to the resonance stabilization, which makes them unbreakable at normal process temperatures (<600°C) until the aromatic character is destroyed by hydrogenation (Gray, 1994).

Table 2.2 Bond dissociation energies

(Data from McMillen and Golden, 1982)

Chemical Bond	Representative bond	Energy, KJ/mol
C-C (aliphatic)	C_2H_5-nC_3H_7	344 ± 4
C-H (primary)	C_2H_5-H	411 ± 4
C-H (secondary)	iC_3H_7-H	398 ± 4
C-H (aromatic)	C_6H_5-H	464 ± 8
C-S	CH_3S-C_2H_5	307 ± 8
C-N	C_2H_5-NH_2	342 ± 8
C-O	C_2H_5O-C_2H_5	344 ± 4

Hydrocarbon macro-radicals can still be subject to further bond breakage if thermodynamically and kinetically favored. The free radical split mainly occurs at the β-position to the free radical site, giving the birth to an olefin and a smaller free radical. The β-scission reaction, which is strongly favored in thermal cracking, will continue until a methyl or an ethyl is produced. For example:

$$CH_3CH_2CH_2CH_2CH_2\dot{C}HCH_3 \rightarrow CH_3CH_2CH_2\dot{C}H_2 + CH_2{=}CHCH_3 \quad (2\text{-}1)$$

$$CH_3CH_2CH_2\dot{C}H_2 \rightarrow CH_3\dot{C}H_2 + CH_2{=}CH_2 \quad (2\text{-}2)$$

where the dot "·" denotes the location of the unpaired electron.

The free radical chain reactions, e.g. thermal cracking of hydrocarbons, consist of three elementary steps: initiation, propagation and termination. Using these steps, Rice and

Herzfeld (1934) first successfully explained the gas-phase thermal cracking reactions of several organic compounds such as ethane, acetone and dimethyl ether. The mechanism proposed by their work can be described as follows:

Initiation: $M \rightarrow 2R^{\cdot}$ (2-3)

Propagation:

Hydrogen abstraction: $R^{\cdot} + M \rightarrow RH + M^{\cdot}$ (2-4)

β-scission: $M^{\cdot} \rightarrow R^{\cdot} + \text{Olefin}$ (2-5)

Termination: $\text{Radical} + \text{Radical} \rightarrow \text{Products}$ (2-6)

Here M and $M^{\cdot}$ represent the parent alkane and parent radical, respectively; $R^{\cdot}$ and RH are lower alkyl radicals and the corresponding alkanes. LaMarca et al. (1993) developed a mechanism incorporating chain reactions for liquid-phase cracking reactions during coal liquefaction. The mechanisms of hydrocarbon thermal cracking usually involve a set of free radical reactions that are drawn from a relatively small number of reaction families, as reviewed by Savage (2000).

In thermal cracking of bitumen and vacuum residue, the formation of gases and distillates is usually accompanied with the formation of coke. As a by-product, coke is of little market value compared with other oil products; therefore, coke formation needs to be controlled. Coke formation is also responsible for fouling in process vessels and furnaces (Watkinson and Wilson, 1997; Lemke and Stephenson, 1998). Given the significant impact of coke formation on the petroleum refining/upgrading industry, the mechanism of coke formation has been extensively investigated.

2.4 FORMATION OF COKE AND MESOPHASE

In petroleum refining and upgrading, coke is usually defined as a carbonaceous material that is insoluble in aromatic solvents such as benzene or toluene. Therefore, similar to asphaltenes and maltenes discussed earlier, coke is also a solubility class consisting of a complex mixture of components.

The mechanism of coke formation has been a research topic under numerous investigations (Magaril et al., 1968, 1971; Wiehe, 1993; Rahimi et al., 1998). Coke is thought to be produced as a byproduct of thermal cracking of petroleum-based feeds through successive reactions that involve polymerization, condensation, and aromaticity increase, in a direction from the lightest to the heaviest fractions as shown below:

$$\text{Oils} \rightarrow \text{Resins} \rightarrow \text{Asphaltenes} \rightarrow \text{Coke}$$

Banerjee et al. (1986) investigated the kinetics of coke formation from five fractions of four types of bitumen over a temperature range from 395 to 510°C. The five classified fractions were asphaltenes, soft resin, hard resin, aromatics and saturates. They concluded that the coke formation was higher for the feed with higher degree of aromaticity and the order of rate constants for coke formation was as follows:

$$\text{Asphaltenes} > \text{Resins} > \text{Aromatics} > \text{Saturates}$$

It is proposed that coke formation involves formation of a new phase, either by phase separation or flocculation of asphaltenes. Magaril and Aksenova (1968) first theoretically developed the concept of a second liquid phase that they suggested as the coke precursor,

emerging at the early stage of coke formation. Wiehe (1993) proposed a phase-separation model for coke formation during thermal cracking of petroleum residues. According to this model, coke formation occurs via a mechanism that involves the liquid-liquid phase separation of reacted asphaltenes to form a phase that is lean in abstractable hydrogen. During thermal cracking, asphaltenes first crack off their aliphatic side-chains to form asphaltene cores and these cores are initially dissolved in the maltenes. As the conversion is increased, more asphaltene cores are formed while the amount of maltenes decreases. When the relative amount of asphaltene cores and maltenes reaches the solubility limit, the asphaltene cores phase separate to form a second liquid phase, in which asphaltene cores will keep cracking off light fragments and recombine to form toluene-insoluble, solid coke. A schematic representation of his phase-separation model is illustrated in Figure 2-3. Storm et al. (1996) proposed an alternate mechanism of the coke formation. From their point of view, asphaltenes are originally dispersed in oil by a layer of absorbed non-asphaltene molecules. This layer, however, will be destroyed at elevated temperatures well below the temperature at which chemical reactions occur. The asphaltenes then flocculate due to the loss of the protective layer. The asphaltene flocculate is suggested to be the coke precursor in the reacting residue and is what Wiehe's phase-separation model referred as the new phase. Some recent evidence that asphaltenes can melt at elevated temperatures (Gray et al., 2004; Asprino et al., 2005), however, weakened the foundation of Storm's coke formation model.

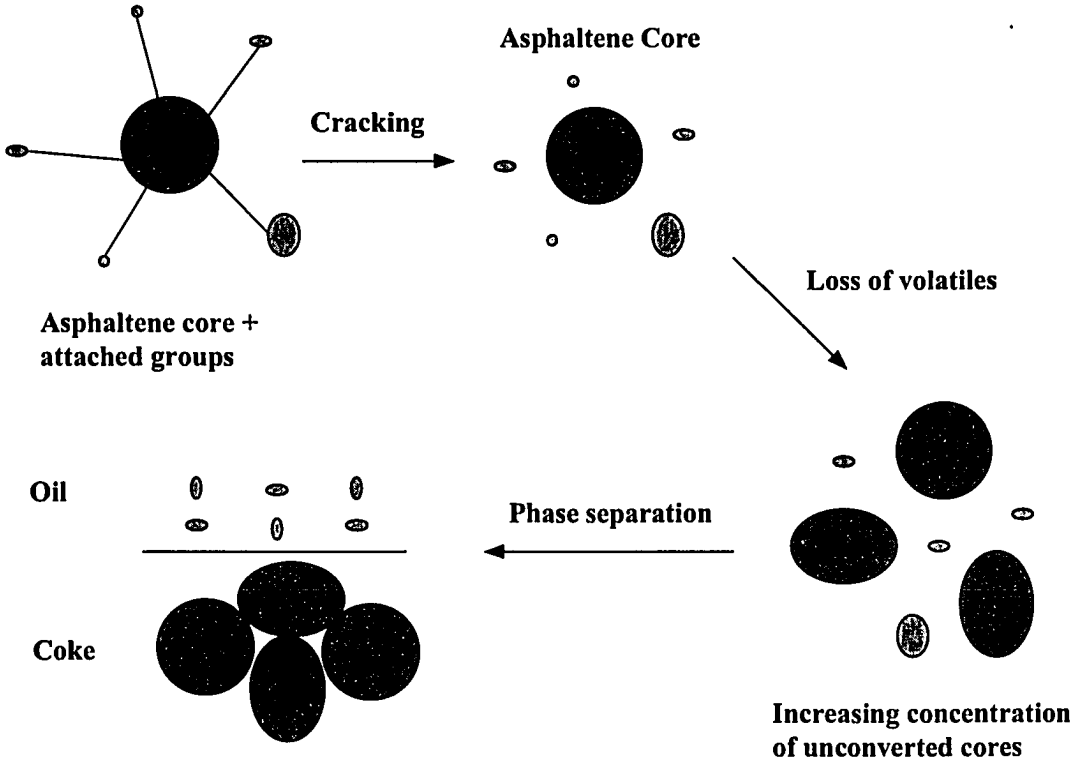

Figure 2.3 Schematic representation of coke formation (after Wiehe, 1993).

During prolonged thermal cracking, the produced coke phase may undergo further physical and chemical changes, and may go through a carbonaceous mesophase stage. Mesophase was introduced to replace the self-contradictory term of liquid crystal (Gray, 1973). Usually, carbonaceous mesophase is observed with optical microscopy as micron-sized spheres during coal tar pitch pyrolysis (Brooks and Taylor, 1965, 1968; Mochida et al., 1988; Korai et al. 1996), and during coking of petroleum residues (Kapustin et al., 1983; Wiehe, 1993; Rahimi et al., 1999). Brooks and Taylor (1965) first observed the thermal transformation of graphitizing carbon to mesophase in the pyrolysis of coal tar pitch. In the earliest stage of thermal decomposition they observed the melting of the original material and the formation of an isotropic pitch-like mass. As the thermal treatment progressed, micron sized spherical bodies were observed which could coalesce and grow with time. The spheres were a manifestation of the separation of a denser second liquid phase, their shape being attributable to the effect of surface tension. These spheres, generally called mesophase spheres, appeared anisotropic under cross-polarized light microscopy, indicating ordering in the liquid structures. Although both coke and mesophase are insoluble in toluene, mesophase is distinguished by its insolubility in strong solvents such as quinoline and its optical properties.

Although coke is accepted as a direct byproduct in coking processes, it is of little market value compared with other oil products; therefore, excessive coke formation is economically undesirable and thus should be controlled. Coke formation is also responsible for fouling in process vessels and furnaces (Watkinson and Wilson, 1997;

Lemke and Stephenson, 1998).

Unlike conventional heavy oils, bitumen extracted from oil sands contains some fine solids, called bitumen solids. Consequently, the effect of fine solids on coke formation is of significantly practical importance to the bitumen upgrading industry.

2.5 FINE SOLIDS AND COKE FORMATION

The hot water extraction process is used commercially to recover bitumen from surface-mined oil sands. During the bitumen separation, some very thin, ultra-fine mineral particles with a major dimension of < 0.3 μm, remain with bitumen. These fine mineral solids are clay particles coated with toluene-insoluble organic matter (Chung et al, 1998; Kotlyar, et al., 1998; Bensebaa, et al., 2000; Sparks et al., 2003). This organic material is polar and aromatic with contributions from both humic and asphaltene-like components. Although toluene-insoluble organic matter dominates the surfaces of bitumen solids, the coverage is patchy rather than continuous. As a result, these solids are capable of stabilizing fine water emulsions in the bitumen phase. The organic matter on the surfaces of the particles has a high propensity to form coke; therefore, these particles can also play a role in fouling on equipment and catalysts. In bitumen upgrading, these solids may be entrained in overhead streams and cause problems in downstream operations.

Fine solids have also shown significant impact on coke formation in thermal treatment of bitumen and heavy oils. Some details of this effect are introduced in the following sections.

2.5.1 Coke Yield

In thermal cracking of bitumen and vacuum residue, the effect of fine solids on coke formation may be directly reflected by the coke yield. Under coking conditions, bitumen solids can have a significant impact on coke yields at short reaction times. Tanabe and Gray (1997) investigated the role of bitumen solids in the coking of Athabasca vacuum residues in a nitrogen atmosphere at 430°C. Compared with the coke yield from solids-free vacuum residue, the presence of bitumen solids in the vacuum residue reduced the coke yield by as much as 7-9 wt% after 20-30 min of reaction, as shown in Figure 2-4. Liu (2002) confirmed the reversibility of this effect, i.e. adding bitumen solids back into the solids-free Athabasca vacuum residue reduced the coke yield correspondingly. Similar to Tanabe and Gray's observation, Liu observed that when bitumen solids were removed from the whole Athabasca bitumen, the coke yield increased. Additionally, coke yield as a function of the concentration of bitumen solids was found to be nonlinear in Liu's study, with the coke yield initially decreasing with increasing concentration, passing a minimum, and then increasing, as shown in Figure 2-5. Sanaie et al. (2001) investigated the effect of mineral additives on coke formation of Cold Lake bitumen at 390 °C. At a level of 2 wt% addition and 4.5 h reaction time, addition of native clays that originally separated from Athabasca bitumen decreased the incipient coke yield by one quarter, from 4 wt% to 3 wt%.

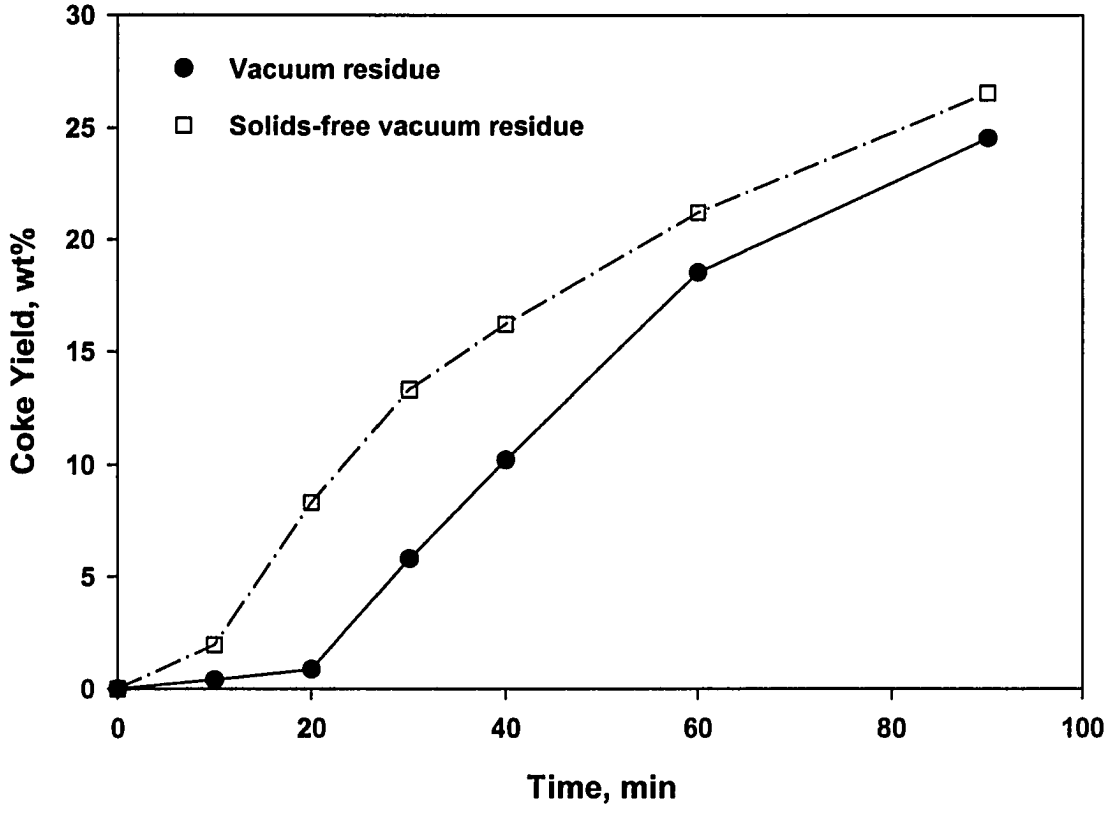

Figure 2.4 Effect of bitumen solids on coke yield of Athabasca vacuum residue under nitrogen at 430 °C (Tanabe and Gray, 1997).

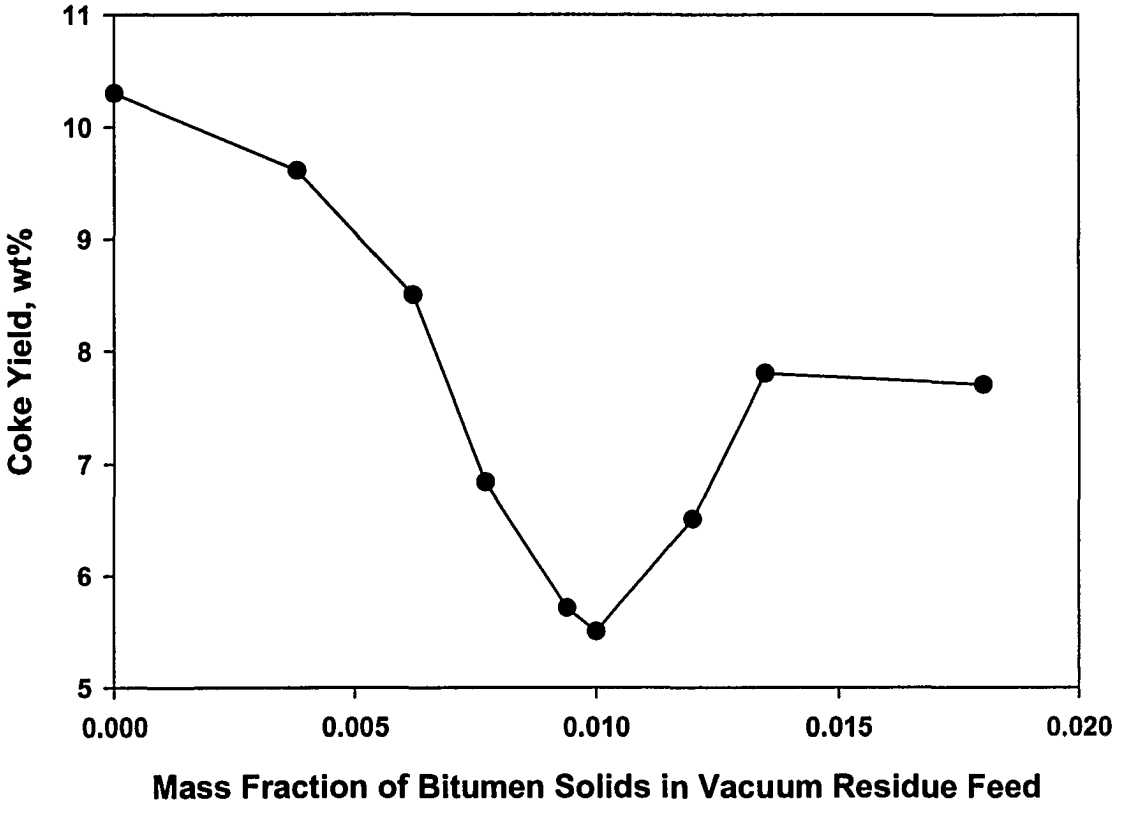

Figure 2.5 Effect of bitumen solids concentration on coke yield in coking of Athabasca vacuum residue at 430°C, N_2 and 20 min (Liu, 2002).

Besides bitumen solids, some other fine additives also showed their capabilities to reduce coke yields during thermal cracking of bitumen and vacuum residue. For example, Liu (2002) found that two foreign fine solids, carbon black and asphaltene-treated kaolin, could reduce the coke yields of solid-free Athabasca vacuum residue under coking conditions. Furthermore, unlike bitumen solids, which gave a minimum coke yield at an intermediate concentration, the carbon black gave a monotonic decrease in coke yield when its concentration was increased to 2.7 wt%.

Some previous studies on the effect of fine solids on coke formation were carried out under hydroconversion conditions. Wolk (1974) patented the use of bitumen solids from oil sands bitumen to suppress coke formation in a hydroconversion process. Nandi et al. (1978) found that adding coal powder to Athabasca bitumen was possible to control coke precursors during hydrogenation reactions. Fouda et al. (1989) investigated the effect of coal addition on petroleum residue reactions with the presence of hydrogen. Increased distillate yields were obtained at low coal concentration without significant penalties in terms of product qualities. The inhibition of coke formation and the enhancement of metals removal were also observed by adding coal in the petroleum residue. For thermal treatment under hydrogen pressure, the observed effects were often attributed to catalytic activity of the solids towards hydrogenation, or synergistic effect between the solids and the hydrogenation catalyst (Attalla et al., 1990; Rosa-Brussin, 1995; Breen et al., 1997). In the case of thermal cracking without hydrogen, Liu (2002) suggested that such catalytic mechanisms were unlikely.

2.5.2 Induction Time and Kinetic Effects

A characteristic of coke formation in bitumen or residue is an induction period during which thermal cracking occurs but no coke is formed. The induction period has been experimentally observed by many previous investigators using a variety of feeds and under different coking conditions (Magaril and Aksenova, 1968; Schucker et al., 1980; Savage et al., 1985, 1988; Wiehe, 1993; Srinivasan and McKnight, 1994). The liquid-liquid phase separation model of coke formation by Wiehe (1993) explained the induction period, by suggesting the coke would form as a second phase only after the solubility limit was exceeded.

In thermal cracking, the presence of bitumen solids in Athabasca bitumen and its vacuum residue could alter the induction period and in turn, the initial kinetics of coke formation. Tanabe and Gray (1997) observed that the Athabasca vacuum residue gave an induction time of 10-15 min at 430 °C before appreciable amounts of coke were formed, but removal of the solids eliminated or deduced this induction time. From a kinetic point of view, the effect of bitumen solids on coke formation was more pronounced at intermediate reaction times of 20-30 min. This effect, however, became unremarkable at prolonged reaction time. For example, after 90 min of reaction, the two feeds gave similar coke yields, although the yield from the solids-free feed was slightly higher, as indicated by Figure 2-4. Liu (2002) found that coking of Athabasca bitumen gave an induction time of about 10-15 min, before which no coke was formed. For the coking of solids-free Athabasca bitumen, there was no induction time and coke formed immediately at the beginning of the reaction.

In Liu's study, bitumen solids showed a similar effect on the initial kinetics of coke formation, which was consistent with Tanabe and Gray's work. Both studies used 0.22 μm Millipore filters to determine coke yields, therefore, they used an equivalent definition.

Fine solids also showed their effect on mesophase appearance time during thermal cracking. In an investigation on the interaction of clay additives (kaolinite, illite and montmorillonite) with mesophase formed during thermal treatment of a solids-free Athabasca bitumen fraction, Rahimi et al. (1999) reported that compared with situations where clay mineral additives were absent, slightly prolonged mesophase induction periods were observed when the additives were present. Gentzis et al. (2001) investigated the effect of two soot samples and delayed coke on mesophase formation in thermal cracking of an Athabasca bitumen vacuum bottoms fraction in a hydrogen atmosphere. The addition of the two soots prolonged the mesophase induction period, but the addition of solid coke from a commercial delayed coking operation shortened the induction period.

2.5.3 Phase Behavior and Wettability

Phase behavior plays an important role in coke formation. In thermal cracking of bitumen and vacuum residue, reactions such as cracking and polymerization can lead to incompatibility in the liquid phase (Magaril and Aksenova, 1968; Wiehe, 1993). Wiehe's model (1993) for liquid-liquid phase separation of coke formation was supported by the observation of spherical particles of liquid crystalline mesophase and the preferential conversion of the most associated asphaltenes to coke. Wiehe failed to point out, however,

that at short times the yield of mesophase material is only a small fraction of the total coke yield. Liu (2002) observed that the majority of the coke collected from the coking of Athabasca bitumen and vacuum residue at 430 °C and 40 min appeared to be agglomerate particles of deformed viscous liquid droplets. Separate spheres were also observed, and the separate spheres were even predominant in some areas of the coke samples. Based on solubility behavior and optical properties, Liu (2002) concluded that these spheres were not mesophase.

When fine solids are present in thermal cracking, the developing coke components in the new phase can interact with fine solids in liquid suspension. Several studies have indicated the importance of fine solids in the liquid-liquid behavior of coke formation. Tanabe and Gray (1997) proposed a hypothesis that the clays particles fine solids accumulated at the interface between the oil and the new phase of coke precursor and thus inhibited the coke from coalescence into larger droplets, analogous to the stabilization of oil-in-water and water-in-oil emulsions, as illustrated in Figure 2-6. Wang et al. (1998) studied the interaction of added fine solids with the toluene-insoluble spheres formed from Athabasca coker gas oil under hydrogen pressure. They found that particles such as carbon black and asphaltene-coated kaolin significantly suppressed the formation of the toluene-insoluble spheres. Rahmani et al. (2003) reported that both fine solids and solvents assisted the dispersion of liquid coke spheres in an oil medium.

Wetting involves the inteaction of a liquid with a solid. The wettability of a solid is generally defined as the preference to contact one liquid, known as the wetting phase, in the

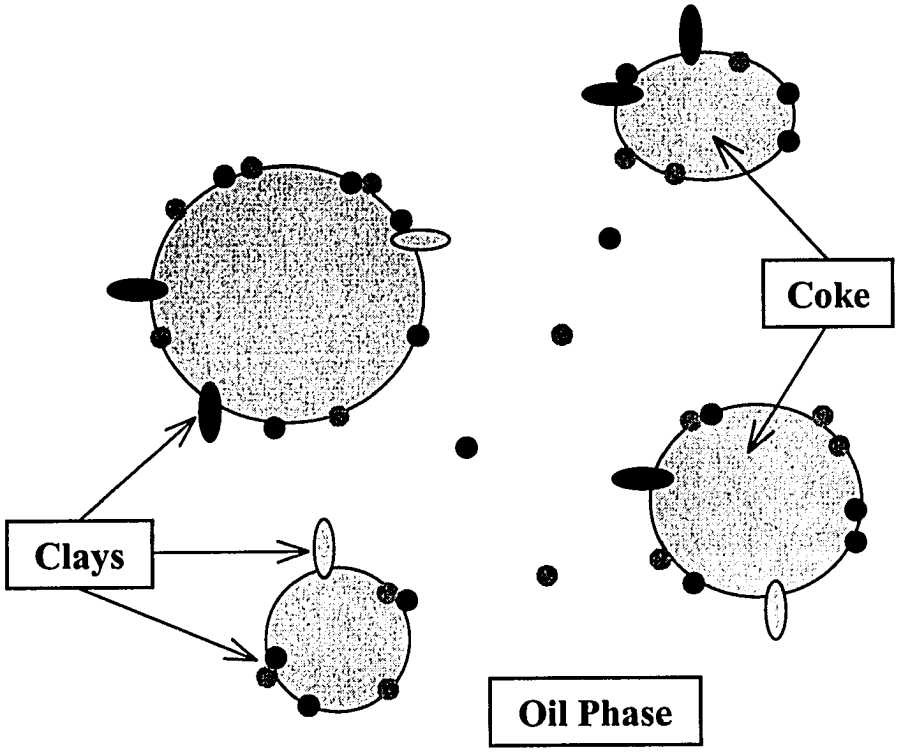

Figure 2.6 Schematic diagram of clays at interfaces of thermoplastic coke dispersed in oil (Tanabe and Gray, 1997).

presence of a second phase. The two terms, hydrophilic and hydrophobic, are used to help characterize surfaces qualitatively to determine solid/liquid interactions. Contact angle is a quantitative measure of wettability. Wang et al. (1998) found that the interaction between the fine solid additives and the toluene-insoluble spheres depended on the hydrophobicity of the solid surface. Little interaction was observed between toluene-insoluble spheres and kaolin particles with polar surface. Addition of particles with non-polar surfaces (carbon black and asphaltene-coated kaolin), however, suppressed the formation of the separate toluene-insoluble spheres. Sanaie et al. (2001) found that addition of Southern Alberta clay had no effect on the initial coke yield, but native clays separated from Athabasca bitumen reduced the initial coke yield to a certain degree. A hypothesis was proposed that the native clays, with their higher carbon content and partially hydrophobic character, disperse much more readily in the bulk oil phase than do the hydrophilic clays and, therefore, interfere more strongly with the developing coke phase.

2.5.4 Particles as Collectors for Coke

During thermal cracking of bitumen and heavy oils, the new coke phase is a second liquid phase formed by polymerization and condensation. This material is likely to wet fine solids with non-polar surfaces. Consequently, hydrophobic fine solids could act as collectors for the new coke phase.

Rahmani et al. (2003) suggested that solids present in the end cut of Athabasca bitumen likely acted as highly dispersed nucleation sites for the coke material, leading to

less coalescence and smaller spheres. In a study of pitch pyrolysis, Méndez et al. (2004) found that the addition of graphite powder slowed polymerization of the pitch components. Evidence from optical microscopy indicated that some mesophase formed during pyrolysis did not appear as single mesophase spheres but as drops attached to the surface of the graphite particles. Korai et al. (1996) proved that the carbon black could absorb on the surface of mesophase spheres, prohibiting their coalescence, leading to smaller size and larger numbers of mesophase spherules.

Liu (2002) proposed a hypothesis that enhanced mass transfer was the cause of reduced coke formation with hydrophobic fine solids. The coke formed initially was a second liquid that could wet and coat the surface of hydrophobic solids to form a thin film, thereby providing a higher mass transfer area and shorter mass transfer path. Enhanced mass transfer facilitated the escape of light hydrocarbon from coke phase and promoted hydrogen shuttling reactions with the hydrogen donor species from the bulk oil phase, leading to a reduced coke formation. Conversely, without dispersed fine solids or with hydrophilic solids, the coke phase tended to form suspended droplets by itself in the bulk phase. Liu's enhanced mass transfer hypothesis was illustrated by Figure 2-7.

Despite the previous studies, the role of fine solids on coke formation has not been well understood. Direct evidence of interaction between fine solids and coke phase during thermal cracking is extremely lacking, which make most proposed mechanisms hypothetical. Further study on the mechanism of fine solids on coke formation is of both

Without solid particle at core:

- Long transport distance

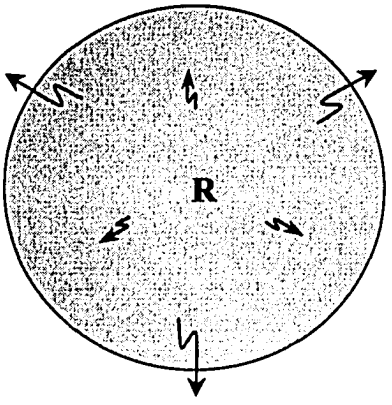

Liquid bulk phase

With solid particle as nucleus:

- Shorter transport distance

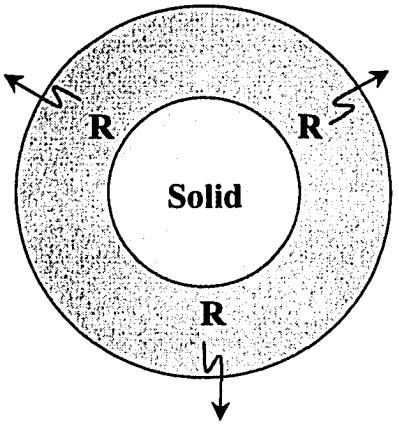

Figure 2.7 Schematic illustration of how hydrophobic solids facilitate mass transfer of light fragments from coke phase (Liu, 2002).

academic and practical importance to determine if this mechanism can be used to enhance industrial coking processes.

3. MATERIALS AND METHODS

3.1 MATERIALS

3.1.1 Oil and Chemicals

In order to study the effect of foreign fine solids on coke formation, a solids-free oil fraction, Arab Heavy Vacuum Residue (AHVR), was used as the feed for forming coke in the coking reaction. The properties of AHVR are listed in Table 3-1.

Table 3.1 Properties of Arab Heavy Vacuum Residue (Syncrude Canada Ltd.)

Property	Arab Heavy Vacuum Residue
Carbon (wt%)	84.1
Hydrogen (wt%)	9.09
Sulfur (wt%)	5.38
Nitrogen (wt%)	0.44
Vanadium (wt ppm)	199
Nickel (wt ppm)	54.3
Microcarbon residue (wt%)	22.8
Asphaltenes (wt%)	19.8
Boiling point distribution (°C)	
10% Mass	523.0
30% Mass	579.5
50% Mass	635.0
70% Mass	700.0

In the coking reaction, AHVR was mixed with a diluent, 1-Methylnaphthalene (1-MN), to control the coalescence of the coke phase formed during the thermal cracking. The 1-MN of 95% purity was supplied by Aldrich (Milwaukee, WI).

1,2,3,4-tetrahydronaphthalene (tetralin) was used as a hydrogen donor in the reaction with toluene-insoluble (TI) products from coking reactions. The laboratory grade tetralin was supplied by Fisher Scientific (Fair Lawn, NJ).

3.1.2 Fine Solid Additives

Two hydrophobic fine solid additives, mesophase carbon and spherical graphite, were used separately as a base for depositing coke, in order to study the formation of coke in a controlled geometry in liquid suspension. The mesophase carbon was supplied by Kawasaki Steel Corp. (Kobe, Japan) and the spherical graphite by BTR Energy Materials Co., Ltd. (Shenzhen, China). Their properties are listed in Table 3-2.

Both the mesophase carbon and spherical graphite showed a high carbon content but very low sulfur content. For the mesophase carbon, despite its reported trace sulfur content (Fukuda et al., 1990), no detectable sulfur content was found by elemental analysis. The mesophase carbon could be regarded as a pure carbon material, given its carbon content of 99.96 wt%.

Table 3.2 Properties of fine solid additives

Property		Mesophase Carbon[a]	Spherical Graphite[b]
Size range (μm)		~ 1-74	~ 6-43
Median size D50 (μm)		17.7	16.8
Specific surface area (m^2/g)		0.46	0.37
Particle density (g/cm^3)		2.23	2.25
Bulk density (g/cm^3)		1.4	1.0
Shape		Irregular	Spherical
	%C	93.1-93.5	99.96
	%H	3.1-2.9	-
Composition	%O	2.0-2.4	-
	%N	1.5-1.0	-
	%S	0.3-0.2	-

[a] The composition of mesophase carbon was taken from Fukuda et al. (1990);

[b] The composition of spherical graphite was provided by BTR Energy Materials Co., Ltd.

3.2 EXPERIMENTAL METHODS

3.2.1 Coking Reactions

Coking reactions were carried out in a 15 ml autoclave batch reactor made from stainless steel tubing and fittings (Swagelok, Edmonton, AB). In this work, all the reactions were run under the standard coking conditions of 430 °C for 40 min, with the reactor initial pressure of 3 MPa nitrogen at room temperature.

In each experiment, 4.5 g of 1-MN was added to the reactor to help control coalescence of the coke phase during the coking reaction. The other reactants, 1.5 g of AHVR and 0.09g of mesophase carbon or spherical graphite, were added to the reactor without premixing. After the reactants were loaded, the reactor was pressure tested and purged with nitrogen three times at 20 MPa. The reactor was closed at 3 MPa nitrogen at room temperature to provide an inert atmosphere. Then the reactor was immersed in a fluidized sand bath (Model SBS-4, Cole-Parmer, Vernon Hills, IL) that was preheated to the target temperature, and agitated at 1 Hz to ensure a uniform temperature during the reaction. After the reaction time had elapsed, the reactor was quenched in cold water to terminate the reaction.

In this work, the stability of the two solid additives in 1-MN was checked under the standard coking conditions. In these blank experiments, no AHVR was loaded in the reactor. Coking reactions on AHVR, with and without solid addition, were conducted to determine the effect of fine solids on coke formation. Each coking reaction was replicated at least three times to ensure the reproducibility. The pathway of coke deposition was also studied by changing the ratio of AHVR to fine solid in 1-MN.

3.2.2 Separation of Products

After quenching of the reactor, the gas was vented and the liquid and solid products were washed out with 60 ml of toluene. The mixture was sonicated for 30 min using an Aquasonic Ultrasonic Cleaner (Model 150HT, VWR, West Chester, PA) to ensure extraction of the liquid product from the solid product. The toluene-insoluble (TI) product, either coke or coke with a fine solid additive, was recovered from the mixture by

filtration using a 0.22 μm membrane filter (Millipore, Billerica, MA). The resultant filter cake was washed with toluene until the toluene passed the membrane without color. To determine the coke yield, the filter cake was weighed after vacuum drying at 70 °C for 12 hours to remove the residual toluene.

The pathway of coke deposition was studied using highly dilute AHVR in 1-MN with fine solid addition. In this case, the liquid and solid products were washed out with 60 ml of toluene and the mixture was kept overnight without sonication. The same filter technique was then used to separate the TI product from the product mixture.

3.2.3 Preparation of Separate TI Particles

In order to examine the interaction between the coke phase and the fine additive, separate TI particles from coking reactions were desired instead of agglomerates. To obtain separate particles, the wet filter cake was redispersed in 15ml toluene right after the filtration and then sonicated for another 2 min. The well-dispersed solid in toluene was put in a shallow glass plate and vacuum dried at 70 °C for 12 hours to remove the toluene. In the study on pathway of coke deposition, the wet filter cake was redispersed in 15 ml toluene without sonication, followed by the same drying process. The dry TI particles that spread on the plate surface were collected for further analysis.

3.2.4 Elemental Analysis

A nitrogen/sulfur analyzer (Model 9000NS, ANTEK, Houston, TX) was used in this study to measure the sulfur content of the original mesophase carbon material, and the

coke material from coking of AHVR in the absence of fine solid addition. The analyzer provided a sulfur analytical range from low ppb to 40 wt%.

3.2.5 SEM and EDX Analysis

Scanning Electron Microscopy (SEM) creates highly magnified images by using electrons instead of light. SEM images have a characteristic 3-dimensional quality and are useful for judging the surface structure of samples. The electron beam in an SEM has energy typically between 5 and 20 keV. An Energy Dispersive X-ray (EDX) analyzer is a common accessory to detect the characteristic X-rays produced when a sample is bombarded with electrons, so that the elemental composition of materials imaged in a SEM can be identified. Elements with an atomic number greater than boron are detected at concentrations of order 1000 ppm. The SEM/EDX technology gives a sampling depth of 1-2 μm and an analysis area with a diameter of 1-5 μm.

In this work, the combination of SEM and EDX was used to examine the particle morphology and characterize the origins of TI materials. Two kinds of solid samples, dry powders and polished cross-sections, were prepared for the analysis. To obtain morphology of separate TI particles, about 2 mg dry powder was spread on a sample holder and sputter-coated with chromium. The sample was then examined under a JEOL (Tokyo, Japan) JSM-6301F SEM. To obtain the cross-sections of separate TI particles and characterize the origins of TI materials, about 20 mg dry powder was well dispersed in a large quantity of lucite powder and underwent a sequence of mounting and polishing. The standard mounting and polishing procedures were attached in the appendices (Part B). The polished surface was sputter-coated with chromium and then and analyzed by the

same SEM with a Princeton Gamma-Tech (Rocky Hill, NJ) EDX analyzer. However, when a line scan on a cross-section sample was required for composition analysis, the 20 mg dry powder was mixed with green bakelite, a more stable dispersant than lucite under the electron beam. After mounting and polishing, the polished surface was sputter-coated with carbon and then analyzed by a Hitachi (Tokyo, Japan) 2700 SEM with a Princeton Gamma-Tech (Rocky Hill, NJ) EDX analyzer.

3.2.6 XPS Analysis

X-ray photoelectron spectroscopy (XPS) is an electron spectroscopic method using X-ray radiation to study the composition and chemical state of the surface region of a sample. The analysis is done by irradiating a sample with soft X-rays (1-2 keV) to ionize atoms and release core-level photoelectrons. The kinetic energy of the escaping photoelectrons limits the depth from which it can emerge, giving XPS its high surface sensitivity. Elements from Li to U are detected at concentrations of order 1000 ppm. For the XPS technology, its sampling depth is 1-10 nm and its analysis area has a diameter of 40 μm to 1 cm.

Samples were analyzed by a Kratos (Kanagawa, Japan) Axis-165 X-ray Photoelectron Spectrometer.

3.2.7 Particle Size Distribution Analysis

In this work, particle size distribution data helped in checking stability of the two fine solid additives and determining the coalescence and agglomeration of the TI phase at the end of coking reactions. All particle size distributions were measured by a Malvern

(Worcestershire, UK) Mastersizer 2000 using laser diffraction technology which could provide a broad measuring range from 0.02 to 2000 μm.

After each reaction, the wet TI product from filtration was dispersed in 10 ml ethanol. Further treatment on the mixture, such as mixing and sonication, might be required before the measurement. The mixture was well stirred to keep it uniform before being sampled into the Mastersizer 2000 for measurement.

3.2.8 Absorbance Measurement

The filtrates from reactions of TI products with tetralin received particular attention. 1 ml of each filtrate was pipetted to a 10 ml volumetric flask and then the flask was filled with tetralin to the graduation. Two quartz cuvettes (dimension: 10mm×10mm×45mm) were used as adsorption cells. One was filled with the dilute filtrate while the other with pure tetralin. The absorbance of the dilute liquid product was measured by a Shimadzu (Kyoto, Japan) UV-160 spectrophotometer under different wavelengths with pure tetralin as a reference.

4. RESULTS AND DISCUSSION

4.1 COKE YIELDS

4.1.1 Blank Experiments with Fine Solids

The stability of mesophase carbon and spherical graphite was checked in 1-MN under the standard coking conditions. In this experiment, no coke was formed because no AHVR was added, and 1-MN was stable under the conditions. Approximately one hundred percent of mass recoveries were obtained for both the mesophase carbon and spherical graphite, with 99.8 % for the mesophase carbon and 99.7% for the spherical graphite. These results indicated that both fine solids were non-reactive in 1-MN under the conditions. Furthermore, both the mesophase carbon and spherical graphite were not friable because the particle size distributions of the mesophase carbon and spherical graphite after the stability checks remained unchanged compared with those of original fine solids (see Table A3-1). The combination of mass recoveries and size distributions confirmed that the two fine solids were stable in 1-MN under the standard coking conditions.

4.1.2 Coking without Solid Addition

When a 25 wt% solution of AHVR in 1-MN was reacted without solid addition, the toluene-insoluble (TI) solid product was attributed to coke. In this case, the coke yield was calculated based on the following formula:

$$\text{coke yield} = \frac{m_{TI}}{m_{AHVR}} \qquad (4\text{-}1)$$

where m_{TI} is the mass of TI product and m_{AHVR} is the mass of AHVR as oil feed.

The average coke yield without solid addition was 9.29 wt%. Repeated experiments showed that the standard deviation of the results was ±0.84 wt% (see Table A1-1).

4.1.3 Coking with Solid Addition

When the 25 wt% solution of AHVR in 1-MN was reacted with the addition of mesophase carbon or spherical graphite, the TI product was a mixture of coke material and the added fine solid. In this case, the coke yield was calculated as the follow:

$$\text{coke yield} = \frac{m_{TI} - m_{additive}}{m_{AHVR}} \qquad (4\text{-}2)$$

where $m_{additive}$ is the mass of the original fine solid additive while m_{TI} and m_{AHVR} are the same as described earlier.

In the presence of fine solids, the average coke yield was 7.15 wt% for the mesophase carbon and 6.29 wt% for the spherical graphite. Repeated experiments showed that the standard deviations of the results were ±0.86 wt% for the mesophase carbon and ±0.23 wt % for the spherical graphite, respectively (see Table A1-1).

In this work, all coking reactions were run under the moderate severity of 430 °C for a short reaction time of 40 min. The coke yields from coking reactions with and without solid addition are shown in Figure 4-1. Compared with the case where no fine solid was added, the coke yield from coking with the addition of mesophase carbon or spherical graphite was reduced by 23 percent or 32 percent, respectively. Consequently, the reduction in coke yield due to the addition of carbonaceous particles was significant. Under similar conditions, Tanabe and Gray (1997) reported that bitumen solids presented in Athabasca vacuum residue could reduce the coke yield by as much as 7-9 wt% after

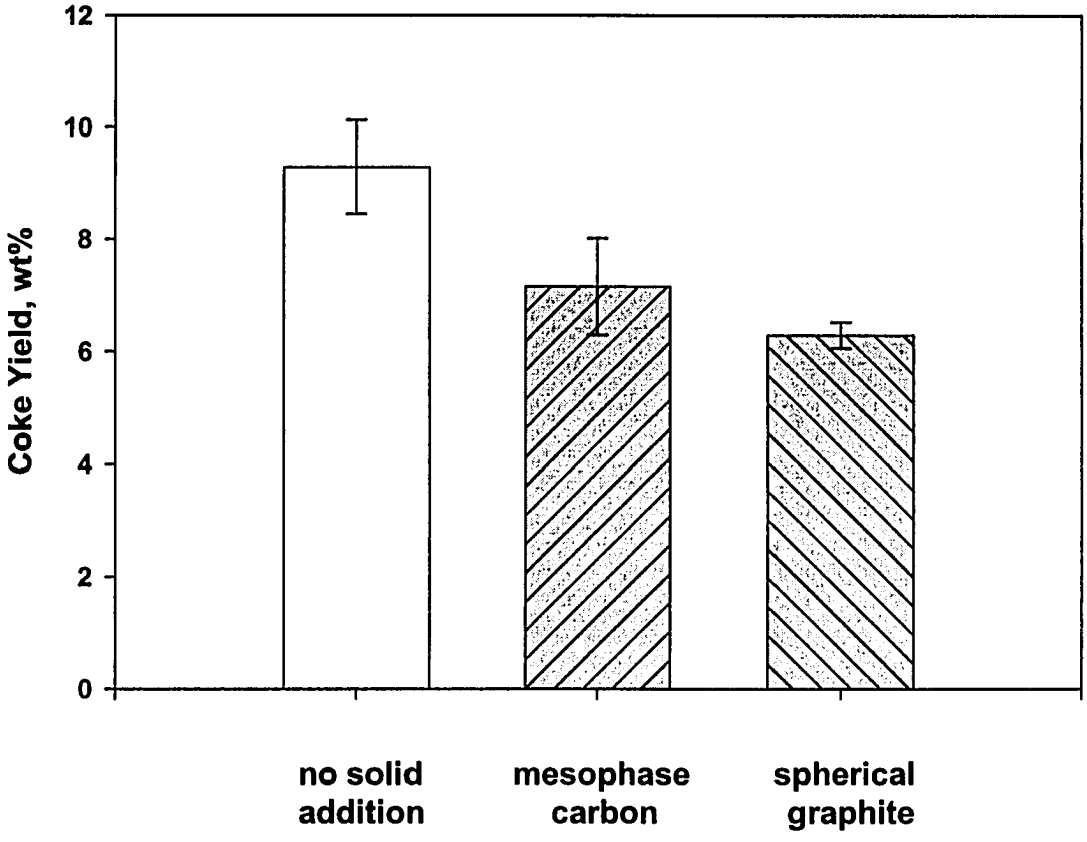

Figure 4.1 Coke yields from 25 wt% AHVR in 1-MN with or without solid addition at 430 °C and 40 min. Carbonaceous particles were added at 0.06 g/g AHVR.

20-30 min when compared with the situation where bitumen solids were removed. Some other investigators (Sanaie et al., 2001; Liu, 2002; Méndez et al., 2004) also observed the same trend in experiments with Cold Lake bitumen, Athabasca bitumen and its vacuum residue, and coal tar pitches. A variety of hydrophobic fine solids were used in their studies, including bitumen solids, carbon blacks and natural graphite. Using AHVR as feed and the mesophase carbon and spherical graphite as foreign solids, this study further confirmed this trend.

From the present results and prior experiments, we concluded that the observation that coke yield is suppressed by hydrophobic solids is quite general for heavy hydrocarbon liquids, and is not unique to a specific feed or type of solid.

4.2 COKE DEPOSITION ON FINE SOLIDS

4.2.1 Morphology of TI Particles

Separated solid particles from the blank experiments and coking of AHVR in 1-MN with and without solid addition were examined by Scanning Electron Microscopy (SEM). Throughout this section, the micrographs show typical particles based on scanning a number of areas of each sample.

The blank experiments on the mesophase carbon and spherical graphite without AHVR gave no coke; therefore, these particles displayed clean carbon surfaces. The mesophase carbon particles, illustrated by SEM micrographs (Figure 4-2), showed angular shapes. Despite the sharp ridges, local areas between these ridges displayed smooth surfaces. Some submicron grains with a variety of shapes and sizes were also sparsely distributed on the surface of larger particles. Compared with the mesophase

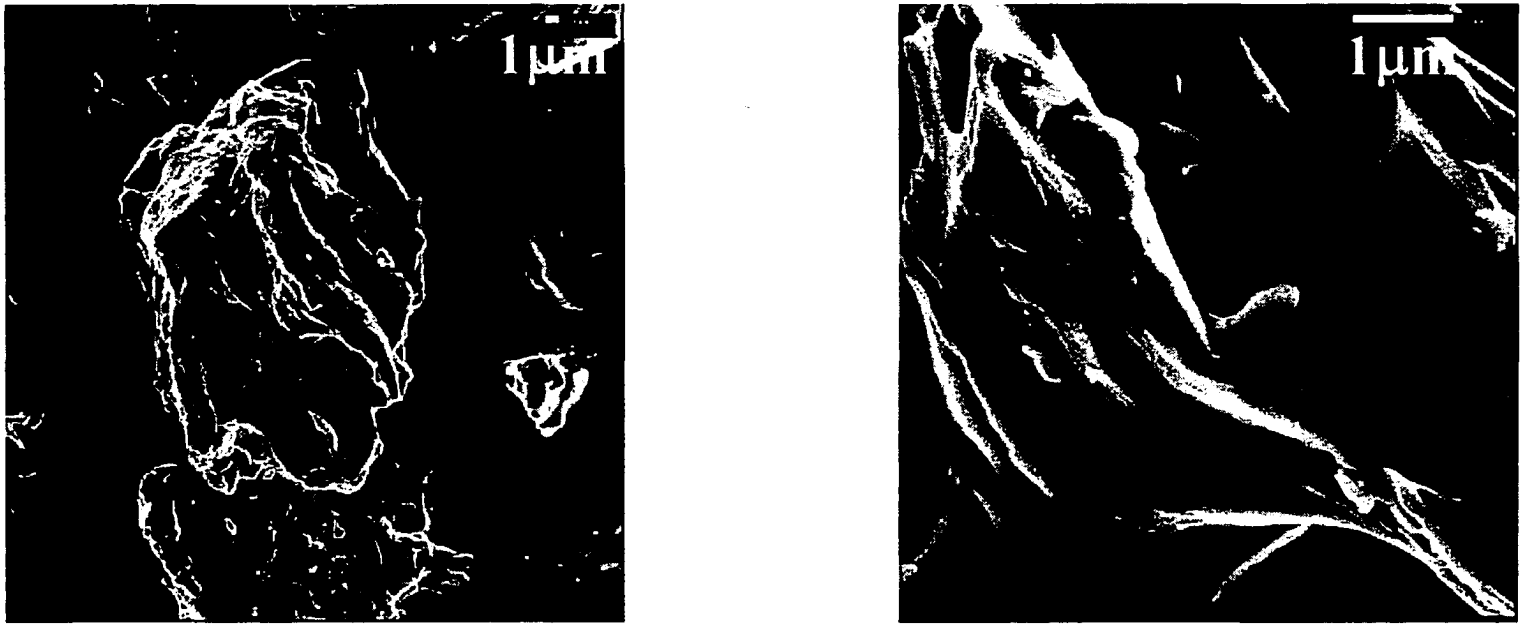

(a) (b)

Figure 4.2 SEM micrographs of a mesophase carbon particle after blank experiment:

(a) a whole particle; (b) a local area in higher magnification.

carbon particles, the spherical graphite particles (Figure 4-3) displayed a more regular shape. The surface was densely covered with overlapped flakes of graphite, giving the particles a compact flaky texture.

The TI product from coking of AHVR without solid addition was coke material. According to the SEM micrographs (Figure 4-4), the surface of the coke particle consisted of submicron spheres. These spheres had evident flowing features with smooth and rounded surfaces. Most small spheres were connected with each other and some even merged into aggregates. Given the broadly distributed small cavities between the linked spheres, the coke particles showed internal porosity.

To minimize the surface energy, a liquid TI phase that is dispersed in a continuous oil phase would be expected to assume the shape with the smallest area and exist as an emulsion of spheres, analogous to oil in water at room temperature. During coalescence, attractive dispersion forces as well as Brownian, hydrodynamic, and surfaces forces act as the driving forces for the droplets to merge, but a high viscosity of the phase existing between the droplets will inhibit the transition to a single spherical droplet (Rahmani et al., 2003).

The TI product from coking with solid addition was a mixture of coke material and the added fine solid. In this case, both coke-only particles and added solid with coke particles were observed by SEM. The latter received particular attention, in order to study the physical interaction between the coke phase and the added fine solid. The mesophase carbon with coke and a particle of spherical graphite with cokes (Figure 4-5 and 4-6) shared some common features in SEM micrographs. Submicron spheres were observed on the surface of both types of particles. Unlike the sparsely distributed grains that

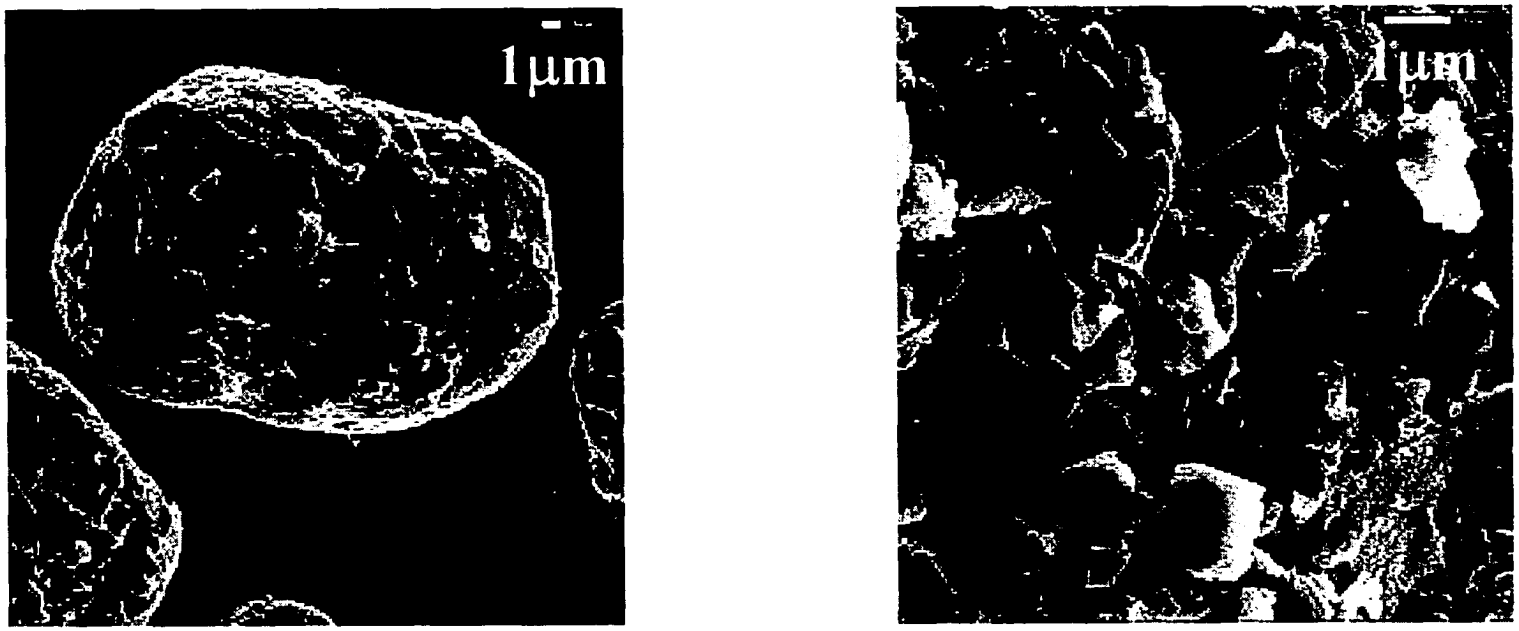

(a) (b)

Figure 4.3 SEM micrographs of a spherical graphite particle after blank experiment:

(a) a whole particle; (b) a local area in higher magnification.

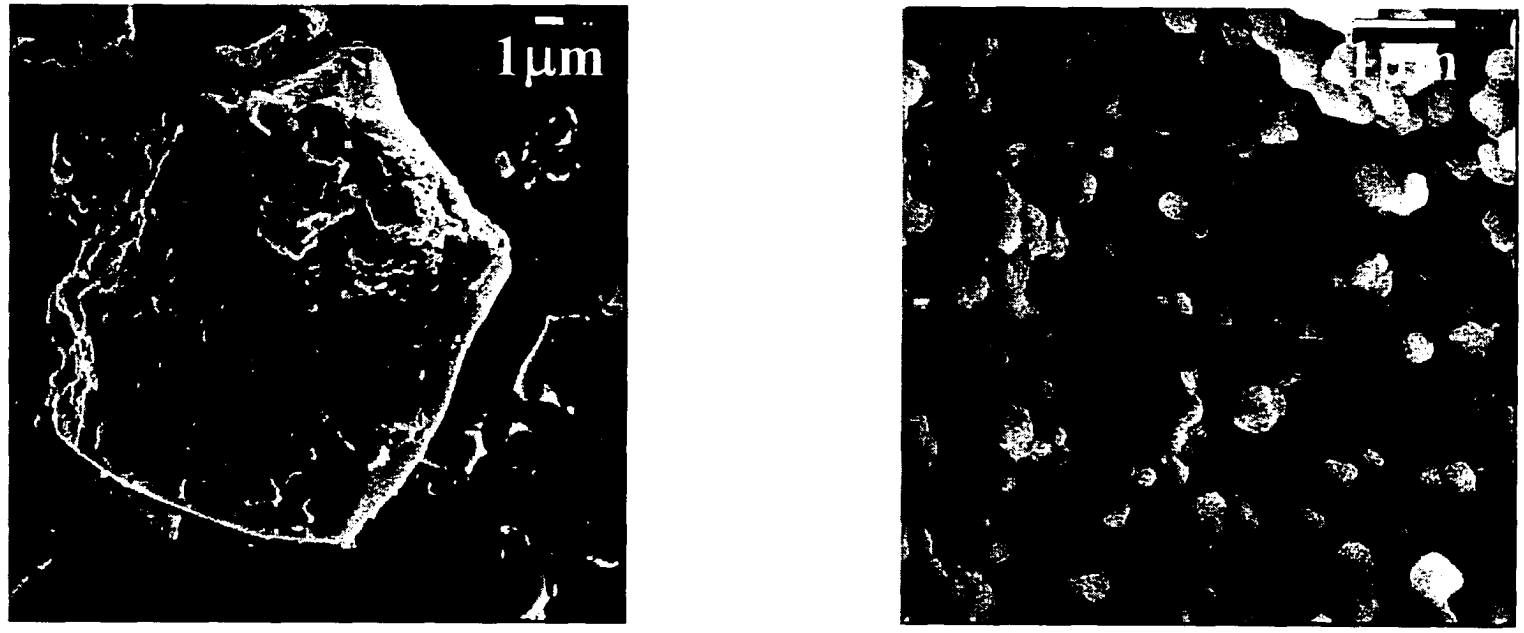

(a) (b)

Figure 4.4 SEM micrographs of a coke particle from 25 wt% AHVR in 1-MN at 430 °C and 40 min:

(a) a whole particle; (b) a local area in higher magnification.

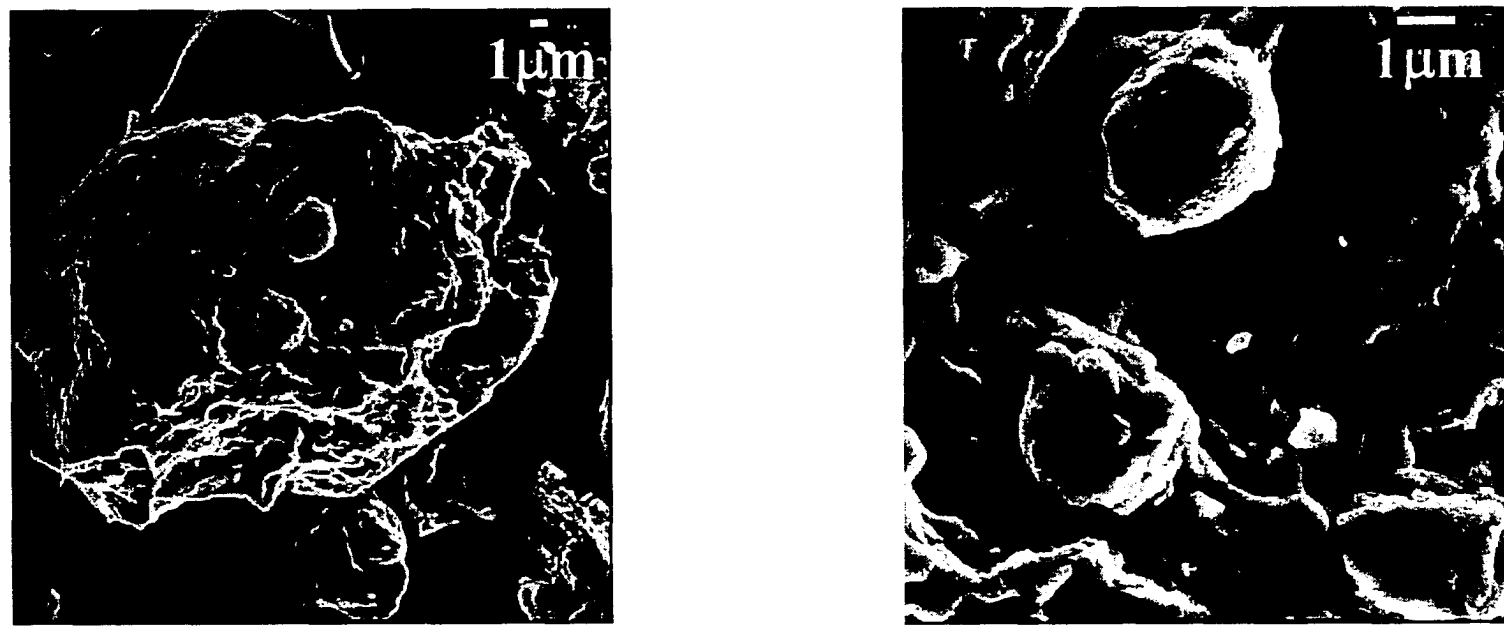

(a) (b)

Figure 4.5 SEM micrographs of a particle of mesophase carbon with coke from 25 wt% AHVR in 1-MN with mesophase carbon addition (0.06 g/g AHVR) at 430 °C and 40 min: (a) a whole particle; (b) a local area in higher magnification.

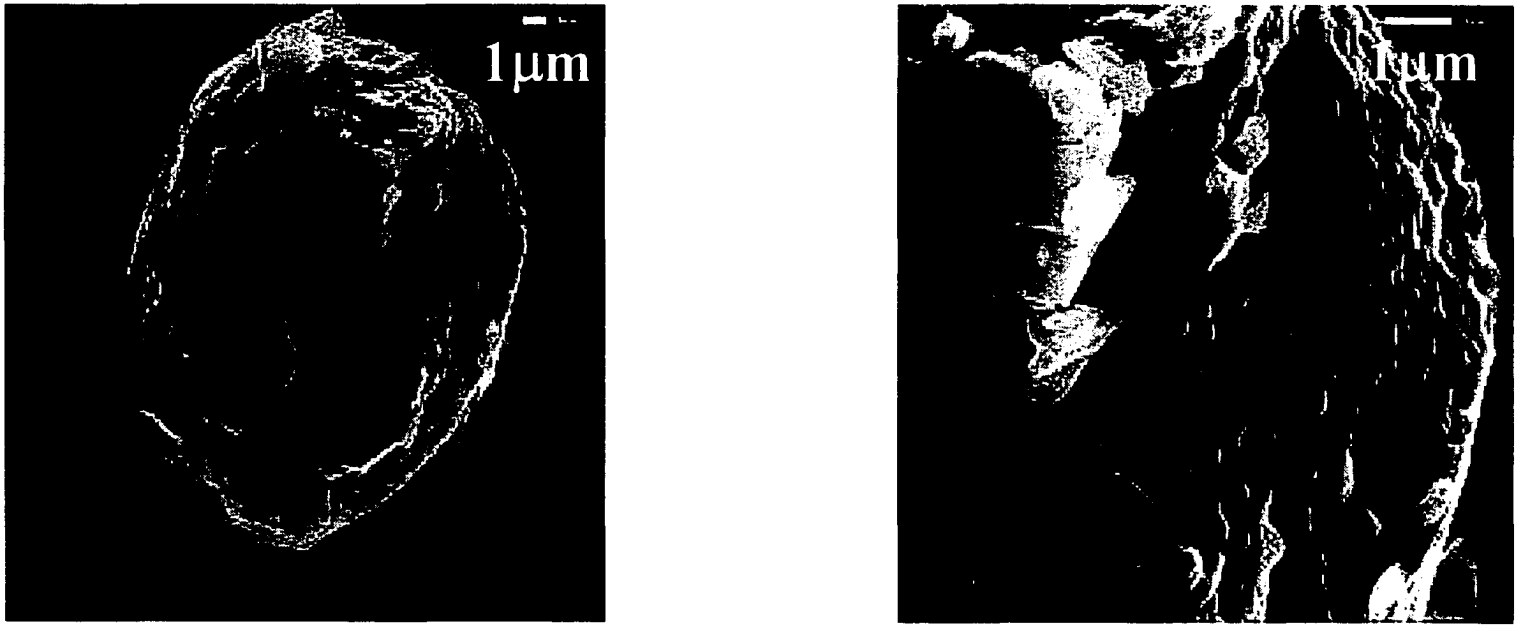

(a) (b)

Figure 4.6 SEM micrographs of a particle of spherical graphite with coke from 25 wt% AHVR in 1-MN with spherical graphite addition (0.06 g/g AHVR) at 430 °C and 40 min: (a) a whole particle; (b) a local area in higher magnification.

appeared on the surface of mesophase carbon particles, these spheres were similar to those that appeared on the coke formed without solid addition (Figure 4-4). These spheres were embedded in a liquid-like layer that probably formed due to the fusion of spheres.

Compared with the mesophase carbon and spherical graphite particles from the blank experiments (Figure 4-2 and 4-3), the morphologies of mesophase carbon with coke and a particle of spherical graphite with cokes (Figure 4-5 and 4-6) were much closer to that of the coke particles without solid addition (Figure 4-4). Given the similarity of TI particles from coking of AHVR with and without solid addition, we suggest that the coke that formed during the coking reactions deposited on the surfaces of the added solids and formed a coke layer. In thermal cracking of coal tar pitches under similar conditions, with graphite added as a foreign solid, Méndez et al. (2004) also observed that the new mesophase did not appear as single mesophase spheres but as drops attached to the surface of the graphite particles. In order to test this explanation for the observed particle morphologies, we examined cross sections of particles.

4.2.2 Cross Sections of TI Particles

Particle cross sections were used to investigate the interaction between the liquid coke phase and the added solids during coking reactions. Micrographs of cross sections of the mesophase carbon and spherical graphite particles (Figure 4-7 and 4-8) showed a compact flaky texture, similar to the surface texture of spherical graphite (Figure 4-3). In contrast, the cross section of a coke particle (Figure 4-9) from the reaction without solid addition, displayed connected submicron spheres and internal voids between spheres. The cross-section structure of coke particles was consistent with the connected agglomerate of

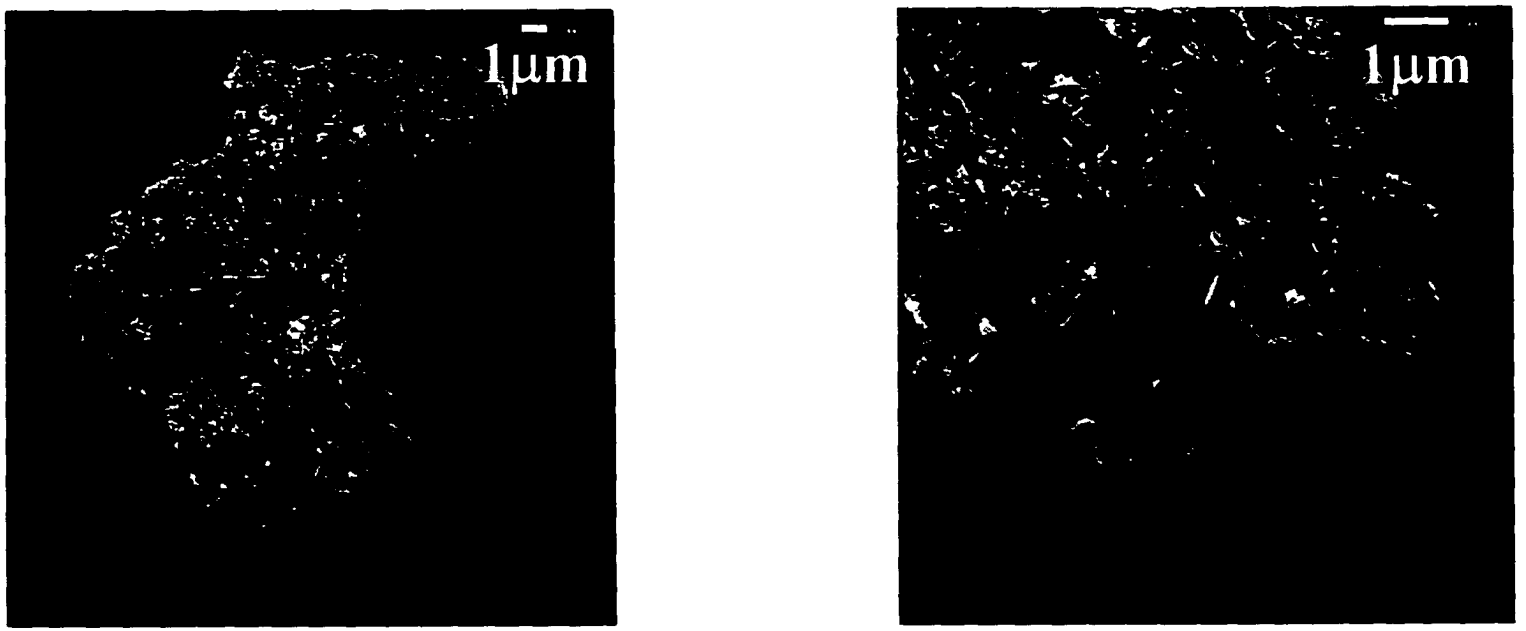

(a) (b)

Figure 4.7 Cross section micrographs of a mesophase carbon particle after blank experiment:

(a) a whole particle; (b) a local area in higher magnification.

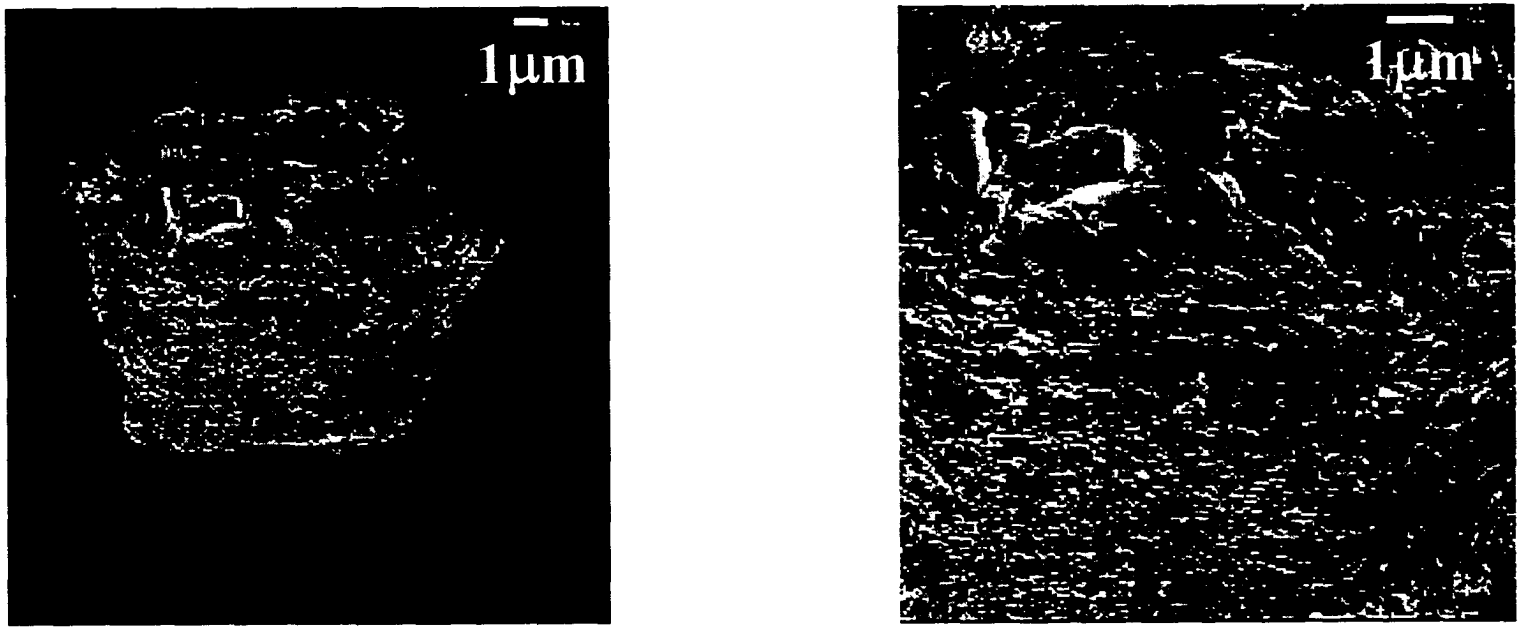

(a) (b)

Figure 4.8 Cross section micrographs of a spherical graphite particle after blank experiment:

(a) a whole particle; (b) a local area in higher magnification.

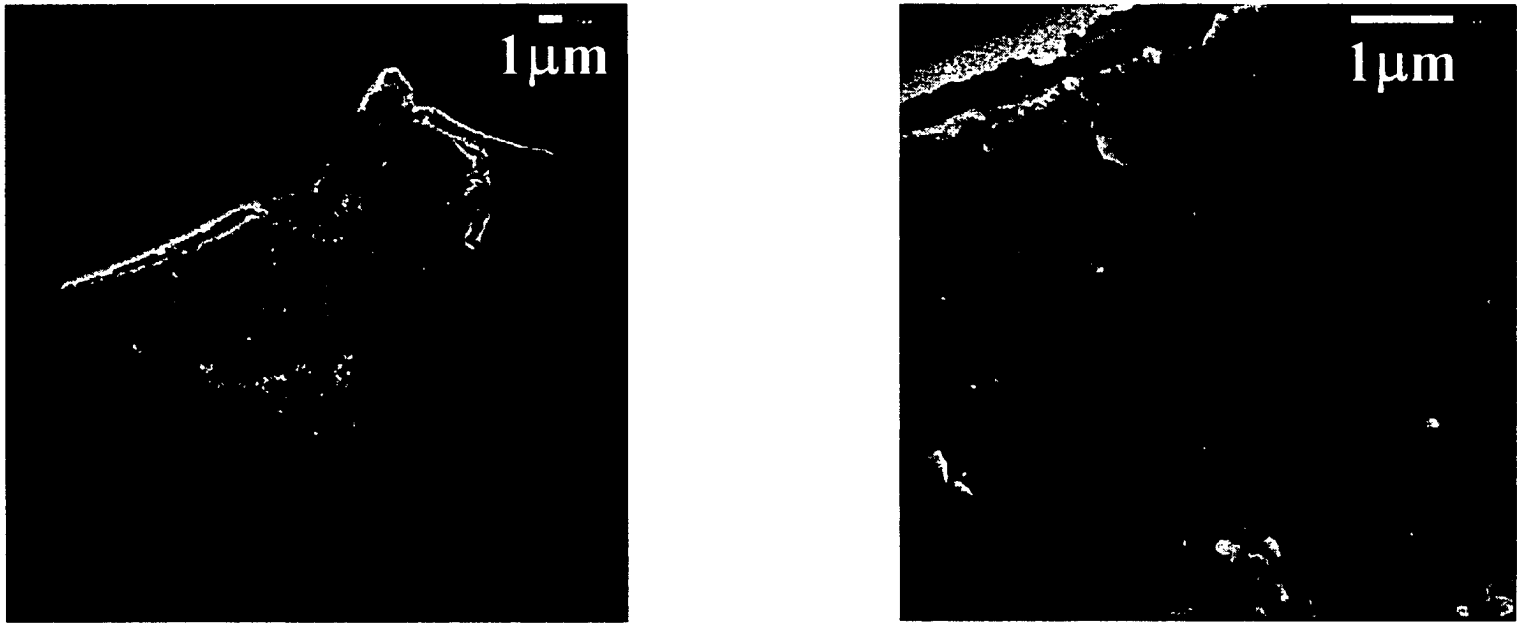

(a) (b)

Figure 4.9 Cross section micrographs of a coke particle from 25 wt% AHVR in 1-MN at 430 °C and 40 min: (a) a whole particle; (b) a local area in higher magnification.

submicron spheres (Figure 4-4).

The cross section of a particle of mesophase carbon with coke (Figure 4-10) displayed two distinctive textures. The central areas showed the typical compact flaky texture as displayed on the cross section of the mesophase carbon-only particle (Figure 4-7), while the edge area showed the typical grainy structure with discrete pores as displayed on the cross section of the coke-only particle (Figure 4-9). The cross section of a particle of spherical graphite with coke (Figure 4-11) also showed the flaky texture in the central area as displayed on the cross section of spherical graphite only particle. In this case, the texture of the edge area was difficult to distinguish in the micrographs, but the interface between the central area and the attached edge area was quite clear. The attachment on the surface of spherical graphite particle was consistent with a new coke phase formed in the coking reaction.

In this work, the coking reactions of AHVR in 1-MN with solid addition were designed to give only a thin layer (1-2 μm) of coke deposition on the added solids, as observed in the cross sections shown in Figure 4-10 and 4-11, although the coke deposits on the solid surface were not of uniform thickness.

In summary, a comparison of the morphologies of TI particles from coking of AHVR in 1-MN with and without solid addition, and their cross sections, suggested that the added solids acted as nucleation centers for deposition the coke phase formed during thermal cracking. The structure of the layers, particularly in Figure 4-10, suggested that submicron particles of coke collected on the surfaces of the carbonaceous particles.

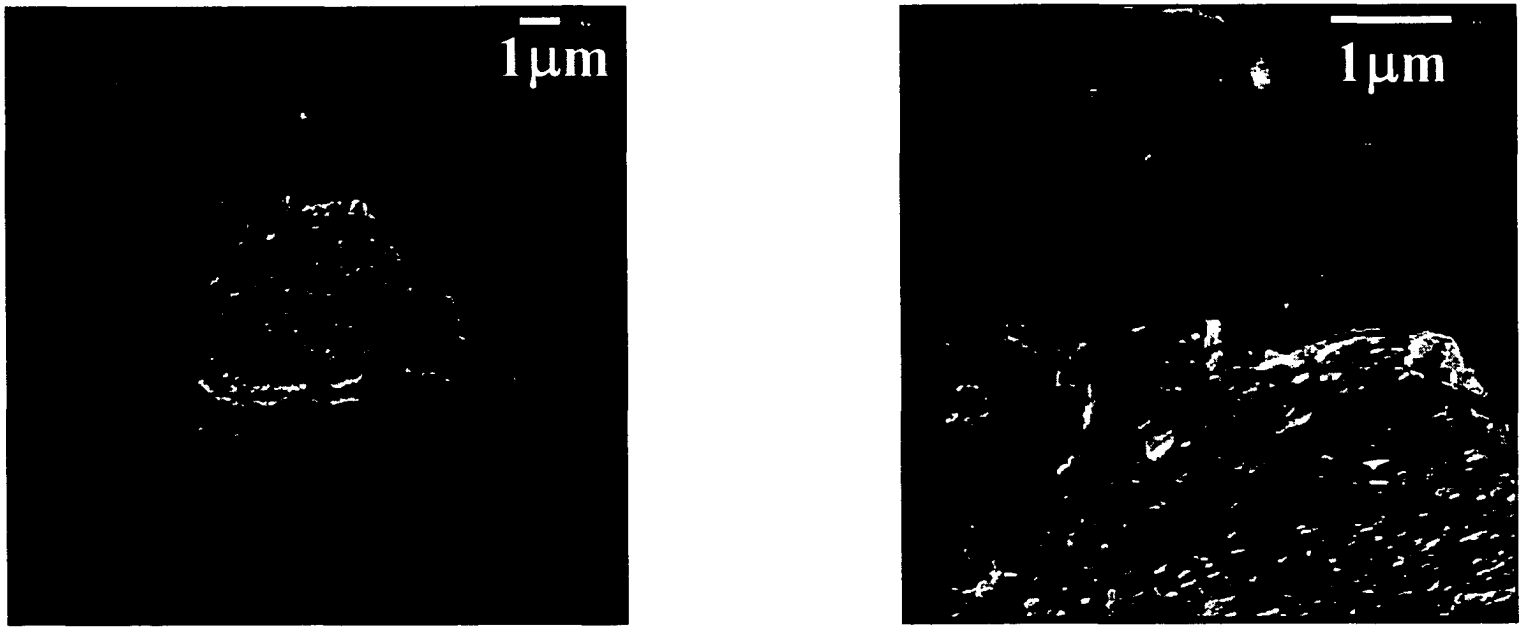

(a) (b)

Figure 4.10 Cross section micrographs of a particle of mesophase carbon with coke from 25 wt% AHVR in 1-MN with mesophase carbon addition (0.06 g/g AHVR) at 430 °C and 40 min: (a) a whole particle; (b) an edge area in higher magnification.

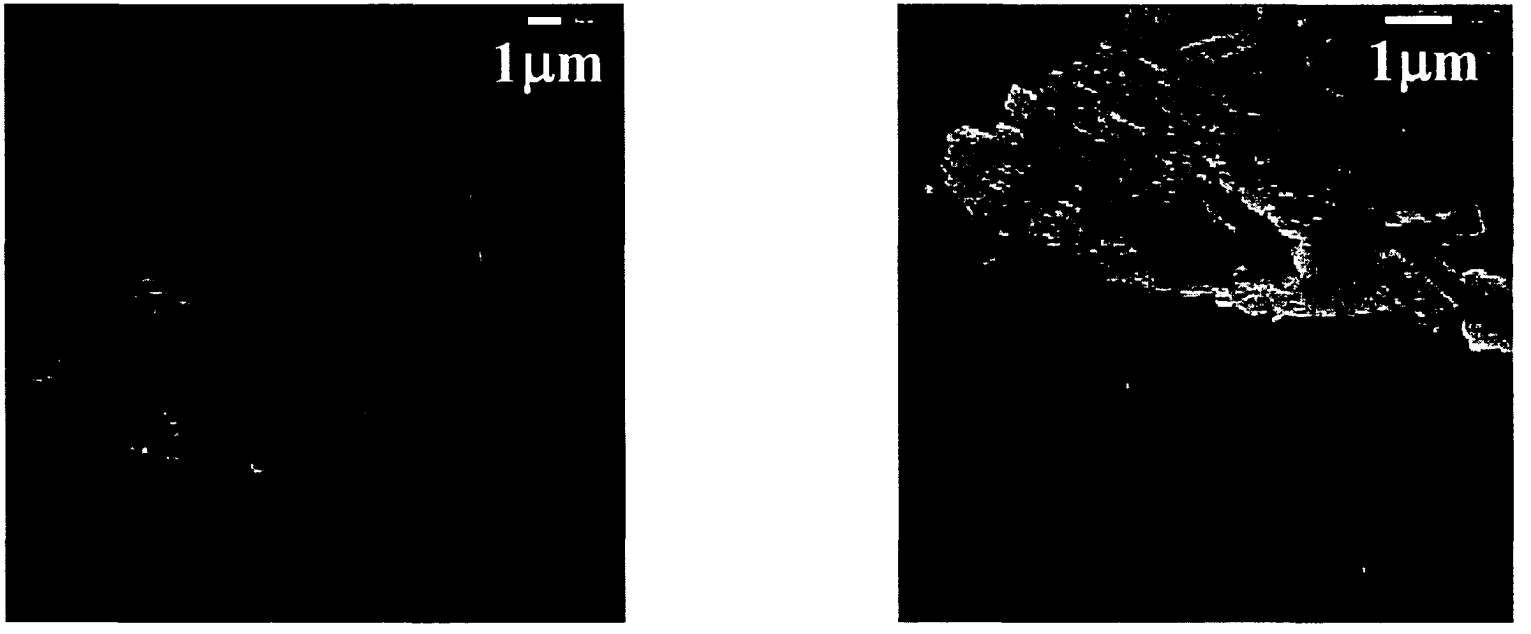

(a) (b)

Figure 4.11 Cross section micrographs of a particle of spherical graphite with coke from 25 wt% AHVR in 1-MN with spherical graphite addition (0.06 g/g AHVR) at 430 °C and 40 min: (a) a whole particle; (b) an edge area in higher magnification.

4.2.3 Chemical Analysis of Coke Deposits

The coke material derived from petroleum-based feeds through thermal cracking contains substantial amounts of heteroatoms such as sulfur and nitrogen. For example, elemental analysis showed that the coke product from coking of AHVR without solid addition contained 7.2 wt% of sulfur (Table A2-1). In contrast, the fine solids used in this work contained almost no sulfur. The spherical graphite could be regarded as a pure carbon material. Despite the traces of sulfur reported by Fukuda et al. (1990) in the mesophase carbon, no sulfur was detected in the material used in this study. Therefore, the difference in sulfur between the coke material and the fine solids could provide contrast for distinguishing the coke deposits from the added solids.

Figure 4-12 shows the results of composition analysis by the Energy Dispersive X-ray (EDX) analyzer on the cross section of a mesophase carbon particle with coke deposits for two small areas: a central and an edge area. The EDX analysis on the central area showed no sulfur signal, which was consistent with the elemental analysis result that the mesophase carbon contained no sulfur. The edge area, however, gave a strong sulfur signal, corresponding to the elemental analysis that the coke material contained certain sulfur. As discussed earlier, the particle morphology suggested that the mesophase carbon particle (Figure 4-12) was coated with a thin layer of coke deposits after the reaction. The compositional analysis of sulfur in the edges and cores of the particles by EDX further confirmed this suggestion.

A line scan for sulfur composition by EDX was also performed on the cross section of both a particle of mesophase carbon with coke and a particle of spherical graphite with coke, as shown in Figure 4-13 and 4-14. Both of the two particles were dispersed in

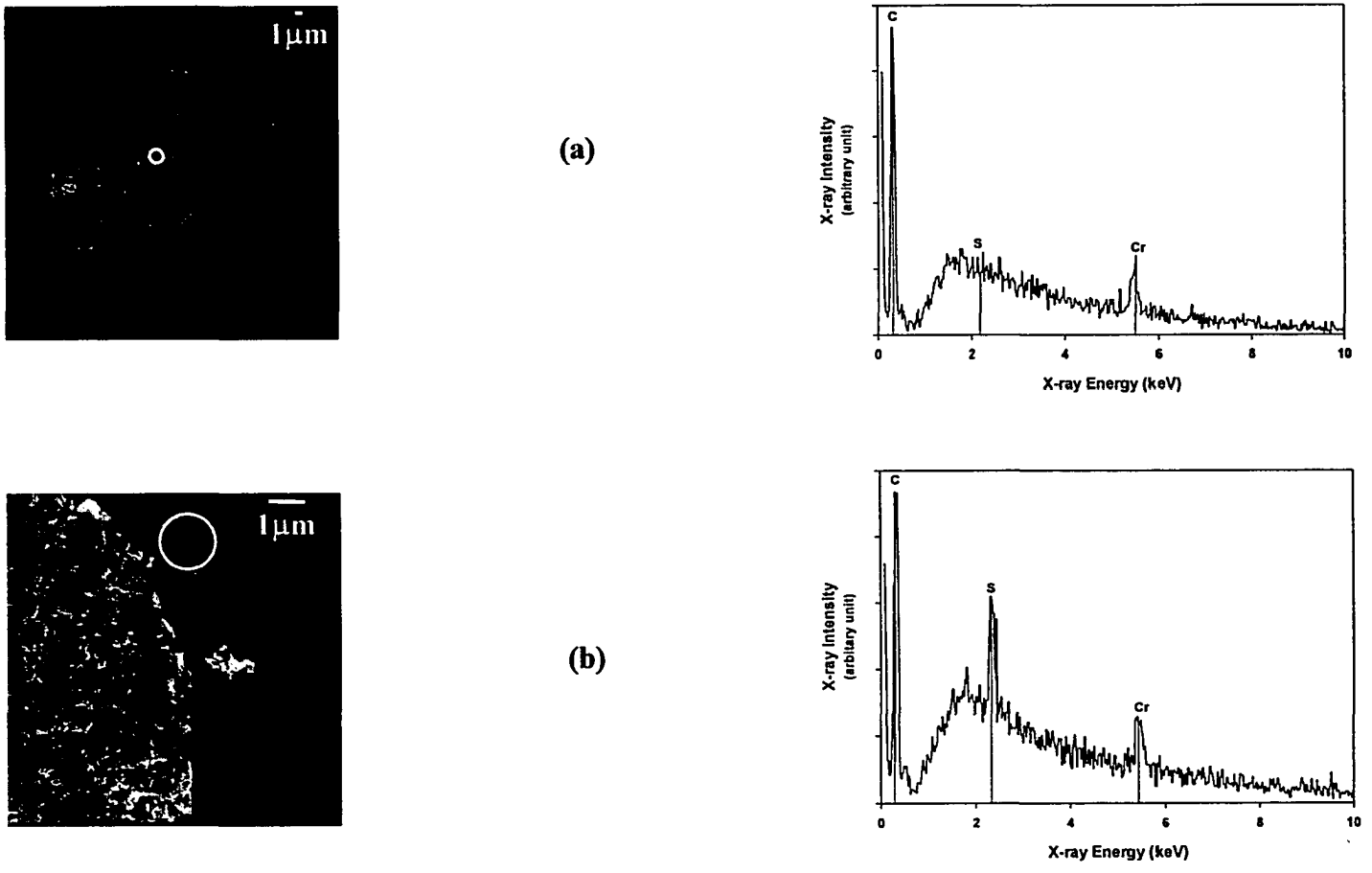

Figure 4.12 Composition by EDX on the cross section of a particle of mesophase carbon with coke:

(a) a central area; (b) an edge area.

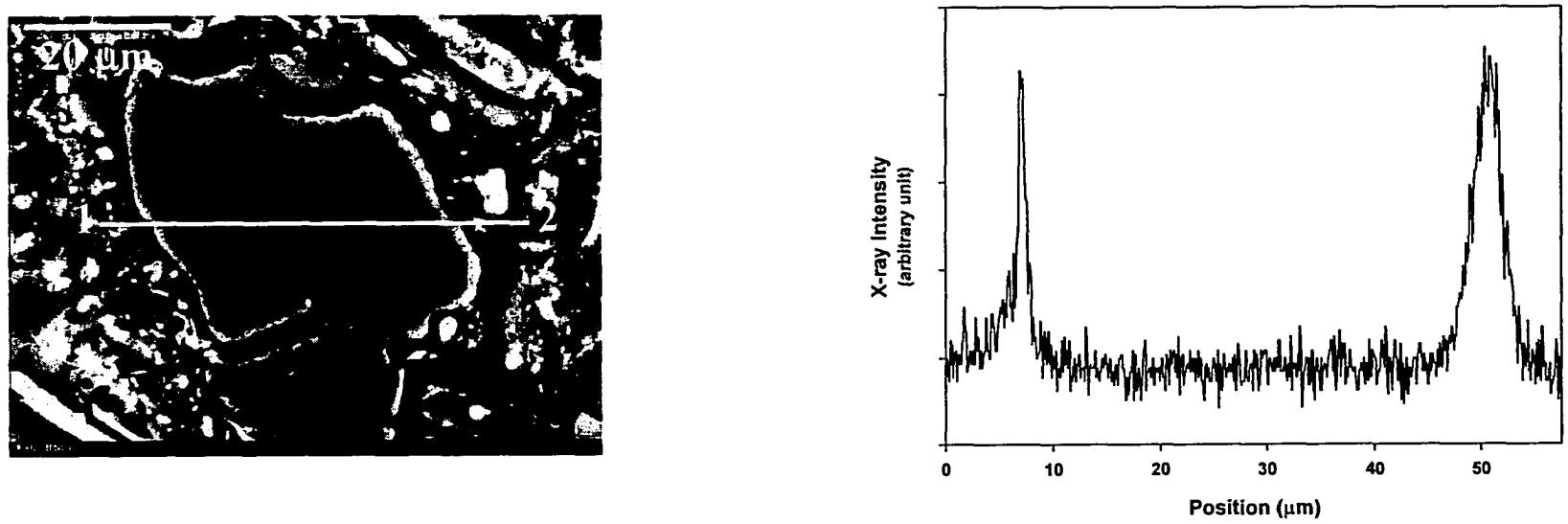

(a) (b)

Figure 4.13 A line scan for sulfur by EDX on the cross section of a particle of mesophase carbon with coke:

(a) cross section of the particle; (b) sulfur signal from point 1 to 2.

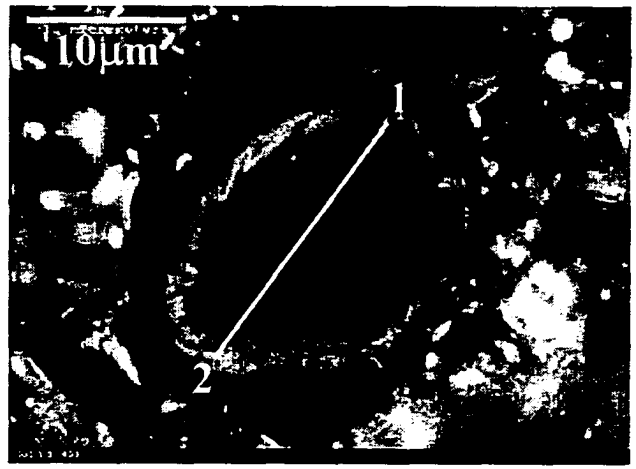

(a)

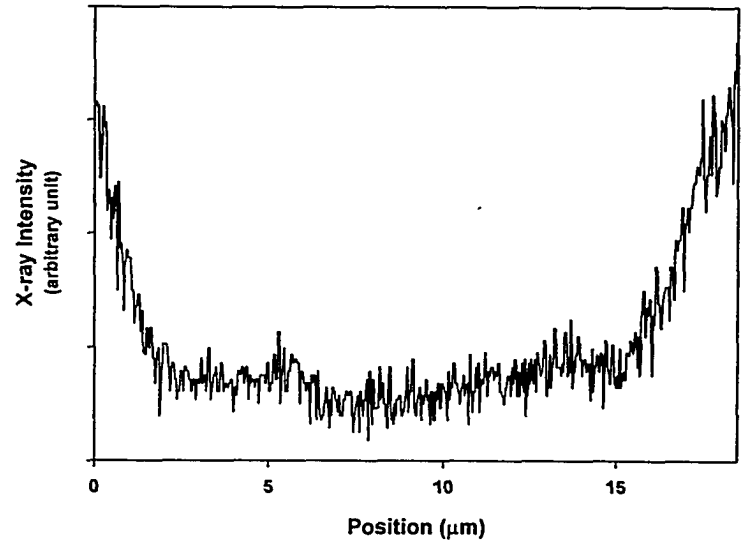

(b)

Figure 4.14 A line scan for sulfur by EDX on the cross section of a particle of spherical graphite with coke:

(a) cross section of the particle; (b) sulfur signal from point 1 to 2.

green bakelite, a material that contained no sulfur. Although the first line scan (Figure 4-13) extended to the particle background while the second one (Figure 4-14) ended at the edge of the particle, all line scans showed strong sulfur signals at the two edges of each particle but very weak sulfur signal in the middle areas. Given the fact that both of the added fine solids contained no sulfur but the coke material from coking of AHVR in 1-MN contained more than seven percent sulfur in weight, it was quite clear that the coke deposits formed a thin layer on the surfaces of the added solids.

In summary, the morphology studies on the TI particles, their cross sections by SEM, and the chemical analysis by EDX provided sufficient evidence to determine the physical interaction between the coke phase and the added fine solids during thermal cracking. All evidence indicated that the highly dispersed carbonaceous particles either acted as nucleation sites for the new coke phase formed in the coking reaction, or that the coke material adhered to surface of the fine solids to form larger agglomerates.

4.2.4 Dependence of Coke Deposition on Coke/Solid Ratio

In this work, the pathway of coke deposition was investigated by keeping the loading of 1-MN and the fine solid constant but changing the loading of AHVR in the coking reactions.

The morphology of the coke deposits suggested two stages of coke formation. The first stage was the formation of coke precursors. The second stage was the agglomeration either of coke spheres to each other or coke spheres on the surface of the carbonaceous

particles. At very low concentrations of coke precursors in the liquid phase, we would expect coke to form directly on the surface of added solids.

To test this hypothesis, the reactor was loaded with highly dilute solution of 0.99 wt% AHVR in 1-MN. In this case, only a very small amount of coke formed under the standard coking conditions. Unlike the connected submicron coke spheres that appeared on the surface of added solids (Figure 4-5 and 4-6), no apparent coke deposition on the added solids was observed in the micrographs (Figure 4-15 and 4-16). Both the mesophase carbon and spherical graphite particles were nearly unchanged compared with those from the blank experiments (Figure 4-2 and 4-3). No sulfur was detected by EDX, likely due to the limitations of EDX as a surface composition analysis method. However, X-ray photoelectron spectroscopy (XPS), a more effective method for analyzing surface composition, gave a surface sulfur content of 4.34 wt% for the mesophase carbon with coke material and 2.88 wt% for the spherical graphite with coke material (Table 4-1). Since both of the two fine solids contained nearly no sulfur, the substantial sulfur content on the surface of each added solid indicated that coke material did deposit on the solid surfaces, although it was not apparent by SEM.

When the reactor was loaded with a solution with an intermediate concentration of 9.9 wt% AHVR in 1-MN, more coke was formed under the standard coking conditions. In this case, the connected submicron coke spheres and their further coalescence and fusion were also observed on both the mesophase carbon and a particle of spherical graphite with cokes (Figure 4-17 and 4-18), similar to those shown in Figure 4-5 and 4-6. Correspondingly, the surface sulfur content increased to 6.39 wt% for the mesophase

carbon with coke material and 5.57 wt% for the spherical graphite with coke material (Table 4-1).

Table 4.1 Surface sulfur content analysis by XPS

Solid sample	AHVR concentration in 1-MN (wt%)	surface sulfur content (wt%)
blank mesophase carbon	_	0.16
blank spherical graphite	_	0.45
mesophase carbon with coke	0.99	4.34
	9.9	6.39
spherical graphite with coke	0.99	2.88
	9.9	5.57

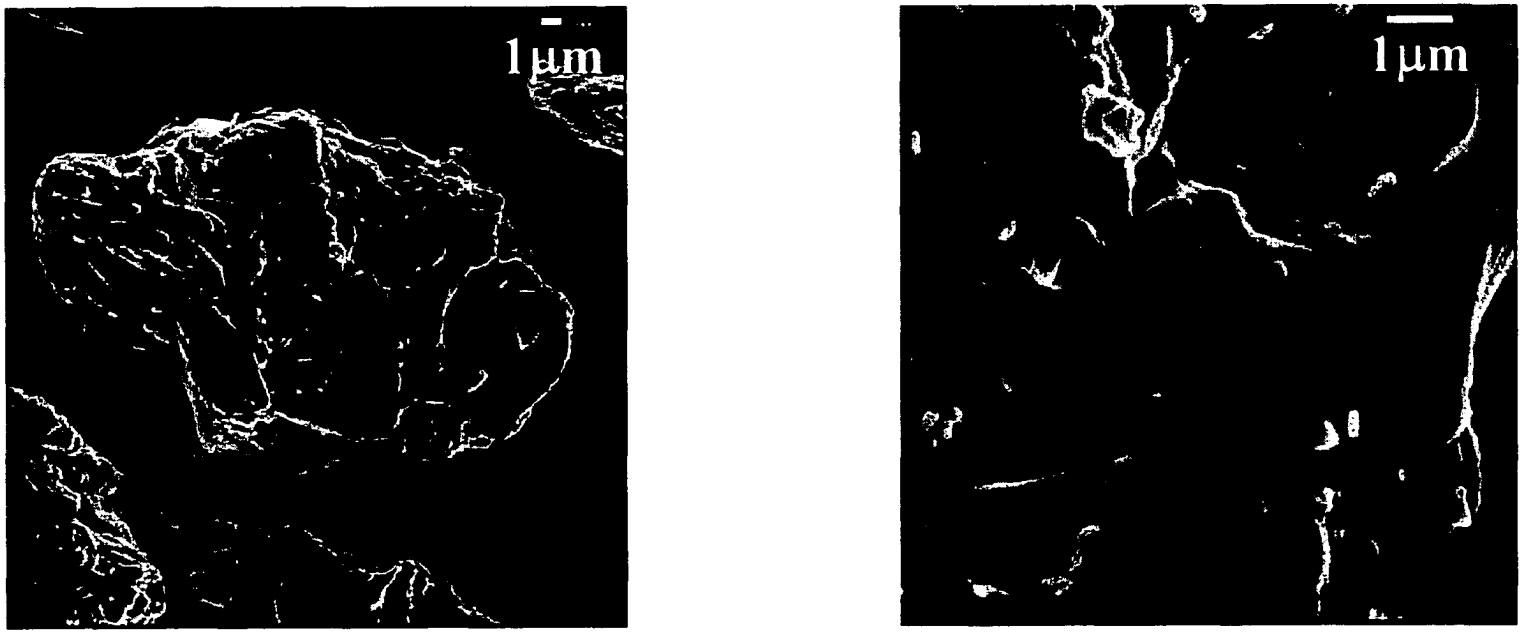

(a) (b)

Figure 4.15 SEM micrographs of a particle of mesophase carbon with coke from 0.99 wt% AHVR in 1-MN with mesophase carbon addition (2.0 g/g AHVR) at 430 °C and 40 min: (a) a whole particle; (b) a local area in higher magnification.

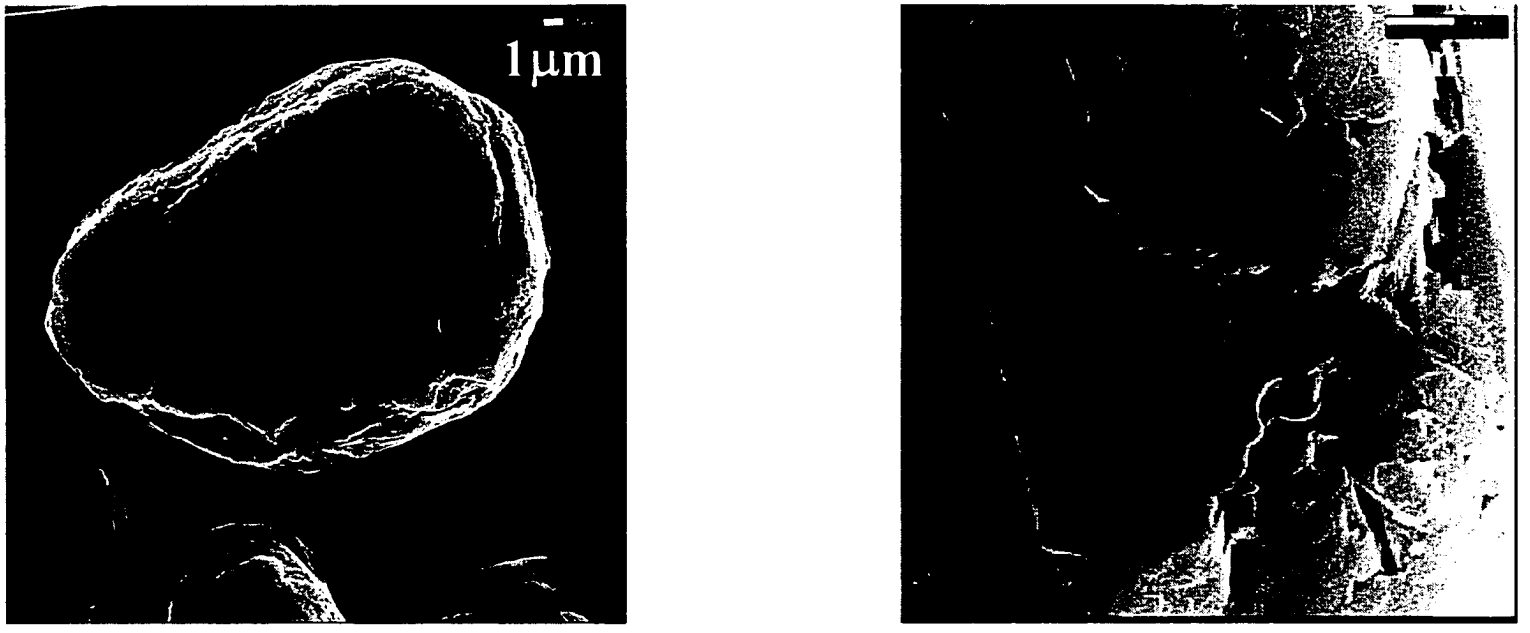

(a) (b)

Figure 4.16 SEM micrographs of a particle of spherical graphite with coke from 0.99 wt% AHVR in 1-MN with spherical graphite addition (2.0 g/g AHVR) at 430 °C and 40 min: (a) a whole particle; (b) a local area in higher magnification.

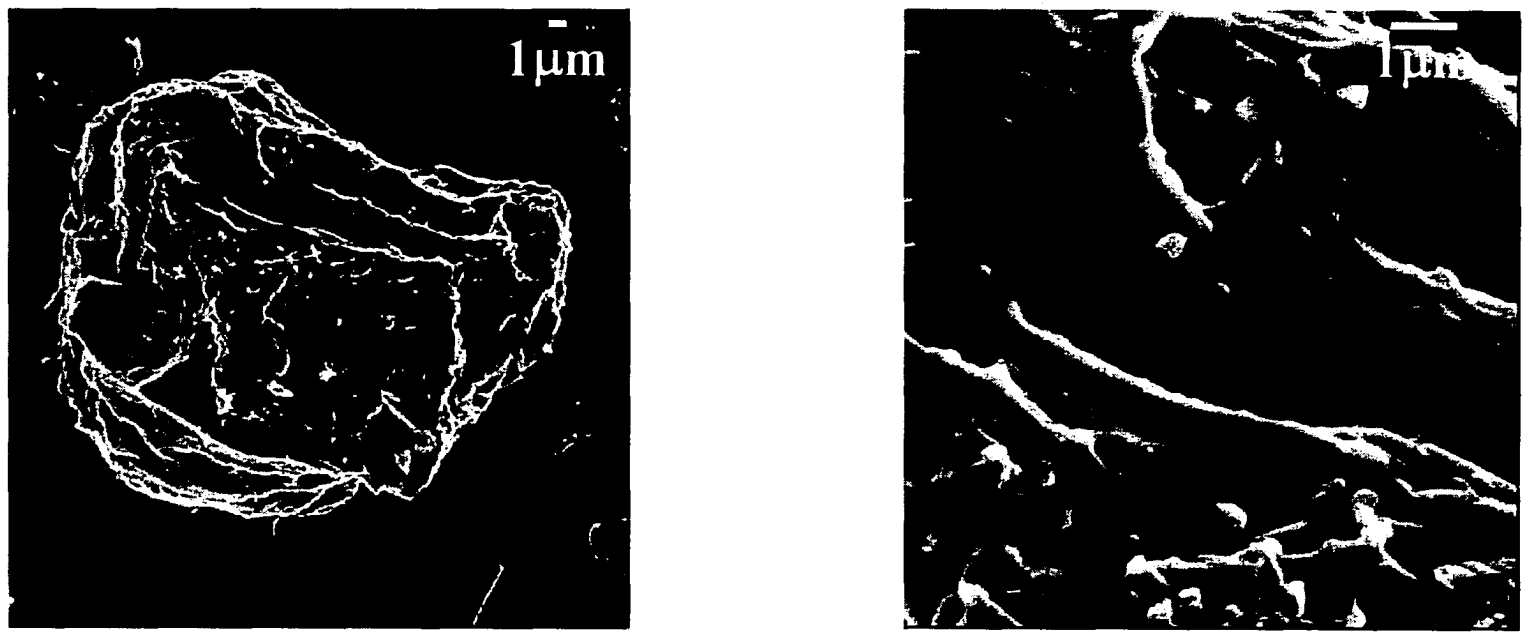

(a) (b)

Figure 4.17 SEM micrographs of a particle of mesophase carbon with coke from 9.9 wt% AHVR in 1-MN with mesophase carbon addition (0.2 g/g AHVR) at 430 °C and 40 min: (a) a whole particle; (b) a local area in higher magnification.

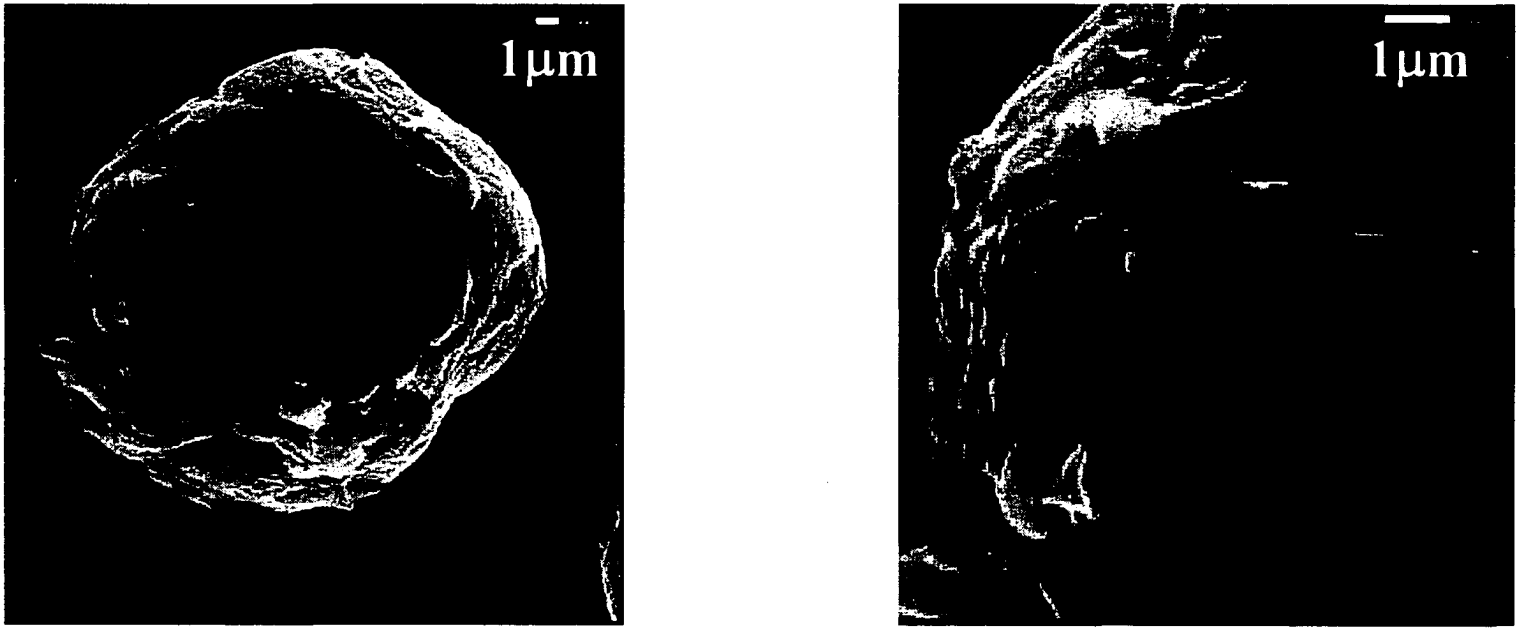

(a) (b)

Figure 4.18 SEM micrographs of a particle of spherical graphite with coke from 9.9 wt% AHVR in 1-MN with spherical graphite addition (0.2 g/g AHVR) at 430 °C and 40 min: (a) a whole particle; (b) a local area in higher magnification.

4.3 MECHANISM OF COKE DEPOSITION ON FINE SOLIDS

The observation of coke layers on the surface of carbonaceous particles over a range of concentrations suggested that the coke deposition mechanism depended on the surface area of hydrophobic fine solids in the liquid phase.

At a very low ratio of AHVR to fine solid, the coke phase deposited directly on the surface of the fine solids in nanometer scale layers, as shown in Figure 4-15 and 4-16. As the ratio of AHVR to fine solid increased, the coke phase appeared to form first in the liquid phase as submicron scale spheres, which then deposited on the added solids. These surface deposits of submicron material subsequently underwent further coalescence and fusion, as shown in Figure 4-5, 4-6, 4-17 and 4-18. At very high ratios of AHVR to fine solid, the coke phase tended to form submicron spheres in the bulk liquid phase and then coalesced and fused, as shown by the coke-only particle in Figure 4-4 as an extreme case.

The mechanism of coke deposition is schematically illustrated in Figure 4-19.

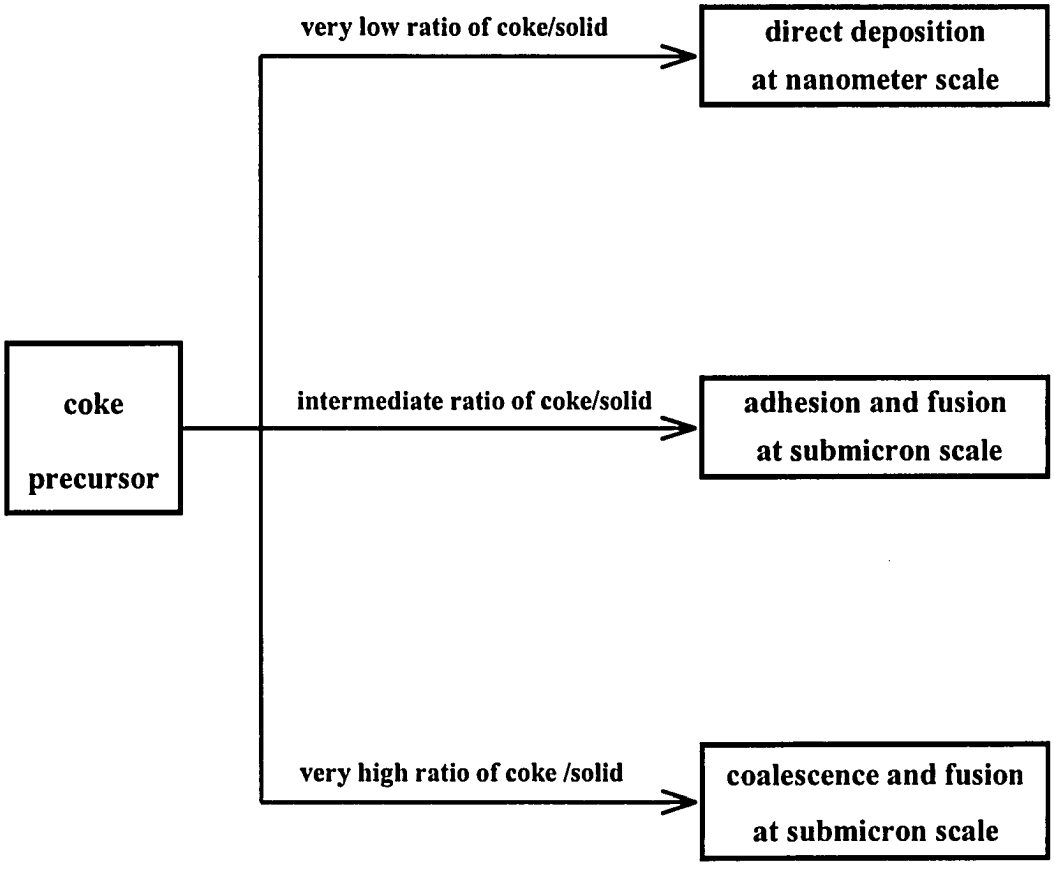

Figure 4.19 Schematic illustration of coke deposition mechanism.

4.4 MECHANISM OF REDUCED COKE YIELD DUE TO SOLIDS

4.4.1 Hypotheses and Experimental Design

Previous studies (Tanabe and Gray, 1997; Sanaie et al., 2001; Liu, 2002) observed the trend of reduced coke yields at short reaction times due to the addition of hydrophobic solids. Using a solids-free oil feed of AHVR and two carbonaceous solids, this study further confirmed this trend. Given the variety of the oil feeds and fine solids used in these investigations, the effect of fine solids on coke formation was quite general. Normally we would expect fine solids to nucleate the formation of a second coke phase during coking reactions, and enhance the TI recovery by filtration, leading to increased coke yields. The reduction in coke yield due to addition of fine solids appears to be "wrong-way" behavior.

What was the mechanism of reduced coke yield due to solids? To answer this question, two hypotheses were proposed: (1) Fine solids dispersed the coke material in the liquid, suppressing agglomeration of the coke phase; (2) Dispersed coke is more accessible to hydrogen donors in the bulk oil phase.

To verify the first hypothesis, the size distributions of two TI products from coking of AHVR in 1-MN were measured by the Malvern Mastersizer 2000. One sample was the coke-only material from coking without solid addition and the other was the spherical graphite particles with coke material from coking with spherical graphite addition. After the TI products were filtered and washed with solvents, they were dispersed in ethanol and shaken for 1 min by a K-500-J Vortex Jr. Mixer (Scientific Industries, Springfield, IL) before the measurements, in order to obtain representative comparison of particle size distributions.

Unlike the industrial coke, which is almost insoluble in everything, the coke formed under the standard coking conditions in this work is very "green". To investigate the interaction of the coke phase with hydrogen donors in bulk oil phase under the coking conditions, TI products from the coking reactions were reacted with tetralin, a well-known hydrogen donor. Tetralin has similar solubility parameter to 1-MN, so the solvent effects would be similar. After the coking reactions of 25 wt% AHVR in 1-MN without solid addition and with spherical graphite addition (0.06 g/g AHVR), each wet filter cake from filtration was mixed with 4.5 g of tetralin and sonicated for 30 min. Each well-dispersed TI product in tetralin was loaded in the same reactor and reacted under the standard coking conditions. After each reaction, the liquid and solid products were separated by the 0.22 μm membrane filter. Each filtrate was collected for the absorbance measurement. The absorbance data was used to monitor the degree of TI conversion during the reaction. The experimental design for TI dissolution in tetralin is illustrated by Figure 4-20.

If the solids enhanced the access of tetralin to the coke material, we would expect the coke dispersed on the graphite particles to be more easily solubilized than the agglomerated coke without graphite particles. Absorbance was used to compare re-dissolution in the solvent after the second reaction with tetralin. The greater the amount of coke solubilized by reaction with tetralin, the larger the absorbance at wavelengths of visible light waves and infrared rays.

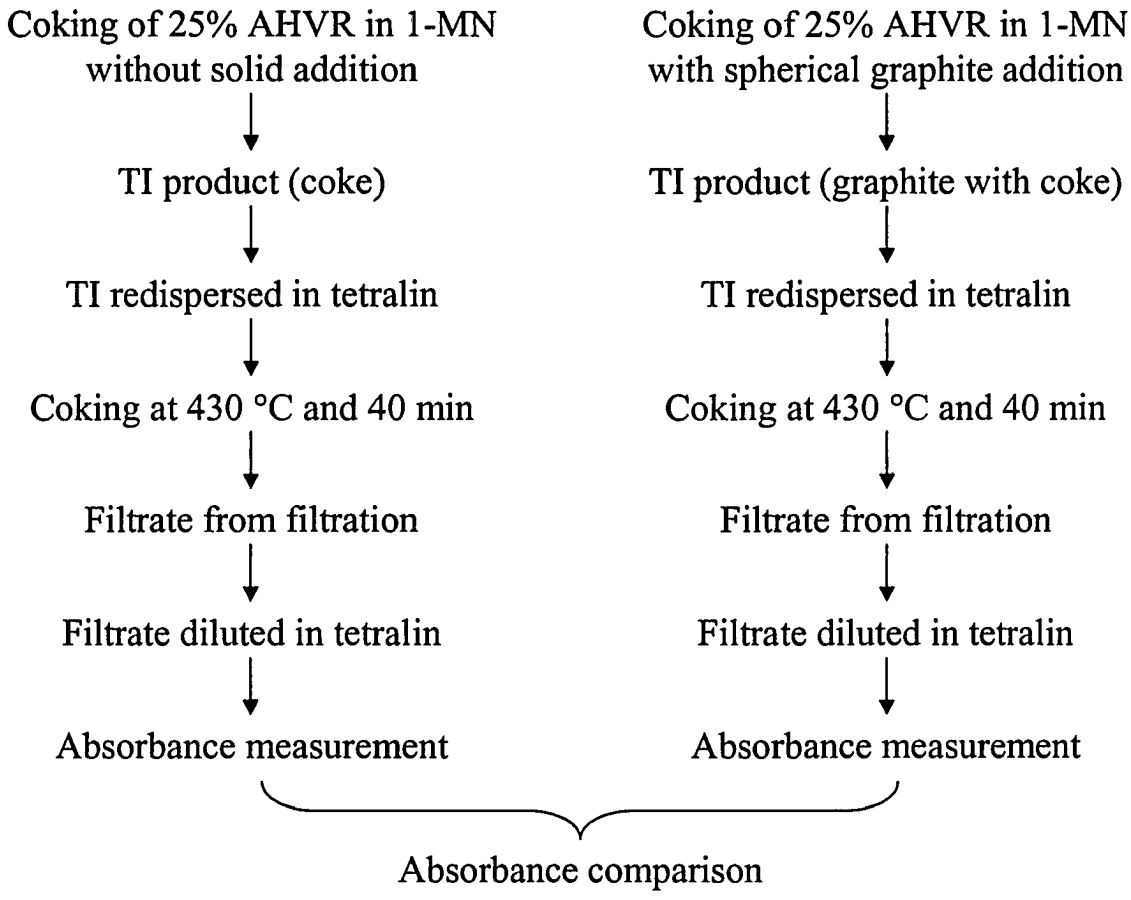

Figure 4.20 Experimental design for reactions of TI dissolution in tetralin.

4.4.2 Particle Size Distributions

The particle size distributions of the two TI samples, together with the particle size distribution of spherical graphite-only sample, are shown in Figure 4-21 (see Table A3-1 and A3-2 for original data).

The coke-only sample had a wider size range, from 0.2 to 550 μm, than the spherical graphite with coke that had a size range from 0.24 to 360 μm. The coke-only sample contained larger agglomerates that were absent in the sample of spherical graphite with coke, which indicated that coking without solid addition gave more coalescence and fusion of the new coke phase during the reaction. For the sample of spherical graphite with coke, a noticeable peak appeared in middle of the distribution due to the added particles. After the coking reaction, the added spherical graphite particles were coated with a thin layer of coke material, as shown in Figure 4-6 and 4-11. The mass moment mean diameter (D_{43}) was 55.8 μm for the coke-only particles, compared to 23.8 μm for the particles of spherical graphite with coke. This result indicated that the presence of spherical graphite did disperse the coke phase in the bulk liquid phase and suppress its agglomeration, compared with the case where the fine solid was absent. The specific areas of the TI particles, however, were similar at 3.0 m^2/g for the coke-only sample and 2.7 m^2/g for the sample of spherical graphite with coke. Based on the data of particle size distributions, the first hypothesis proposed on the mechanism of lower coke yield due to solids was verified. Tanabe and Gray (1997) suggested that fine particles might prevent coalescence of coke droplets during thermal cracking. By comparing the mean diameter of TI particles, several other investigators (Wang et al., 1998; Rahmani et al., 2003) reported the role of clay particles in suppressing the growth and coalescence of coke

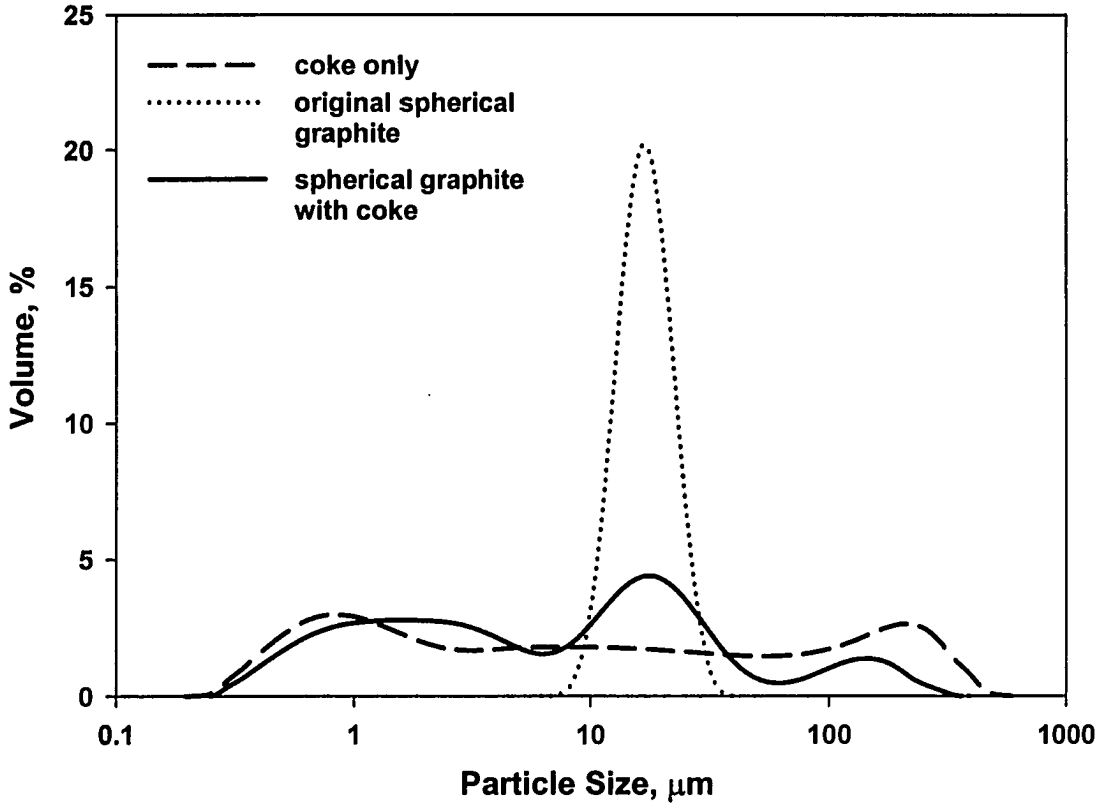

Figure 4.21 Comparison of particle size distributions of TI products from 25 wt% AHVR in 1-MN without solid addition and with spherical graphite addition (0.06 g/g AHVR) at 430 °C and 40 min. TI products were suspended in ethanol and shaken for 1 min.

spheres. Given the evidence from both particle morphologies and size distributions, this study confirmed that fine solids could provide better dispersion for the coke phase in an oil medium by providing highly dispersed nucleation sites for the coke deposits.

From mass transfer point of view, the mass moment mean radius (R_{43}) of the coke material represented the mass transfer distance from the core of coke agglomerates to the bulk liquid phase. The mean radius for the coke-only sample was 27.9 μm. The coke material in the sample of spherical graphite with coke could be divided into two populations: those separate coke particles and those coke deposits on the spherical graphite particles. After correction for the spherical graphite particles, the mean radius for the coke material in the sample of spherical graphite with coke was estimated to be 16.7 μm (see appendices - Part C). Apparently, compared with the coking without solid addition, the coking with spherical graphite addition significantly reduced the mass transfer distance between the coke phase and the bulk oil medium.

Sonication time had a significant impact on the measured size distributions of TI products dispersed in ethanol, as shown in Figure 4-22 (see Table A3-3 for original data). After 30 min of sonication, the coke-only sample gave a size range of 0.2 to 30 μm and the sample of spherical graphite with coke of 0.2 to 40 μm, which indicated that the large coke agglomerates that appeared in Figure 4-20 were broken into small pieces or dispersed due to sonication. The sample of spherical graphite with coke showed a well-separated bimodal size distribution, with one peak being of the coke-only particles and the other the spherical graphite coated with coke particles. The mode was around 0.6 μm for the coke-only particles while 16 μm for the particles of spherical graphite coated with coke. A calculation based on this bimodal size distribution showed that approximately 40

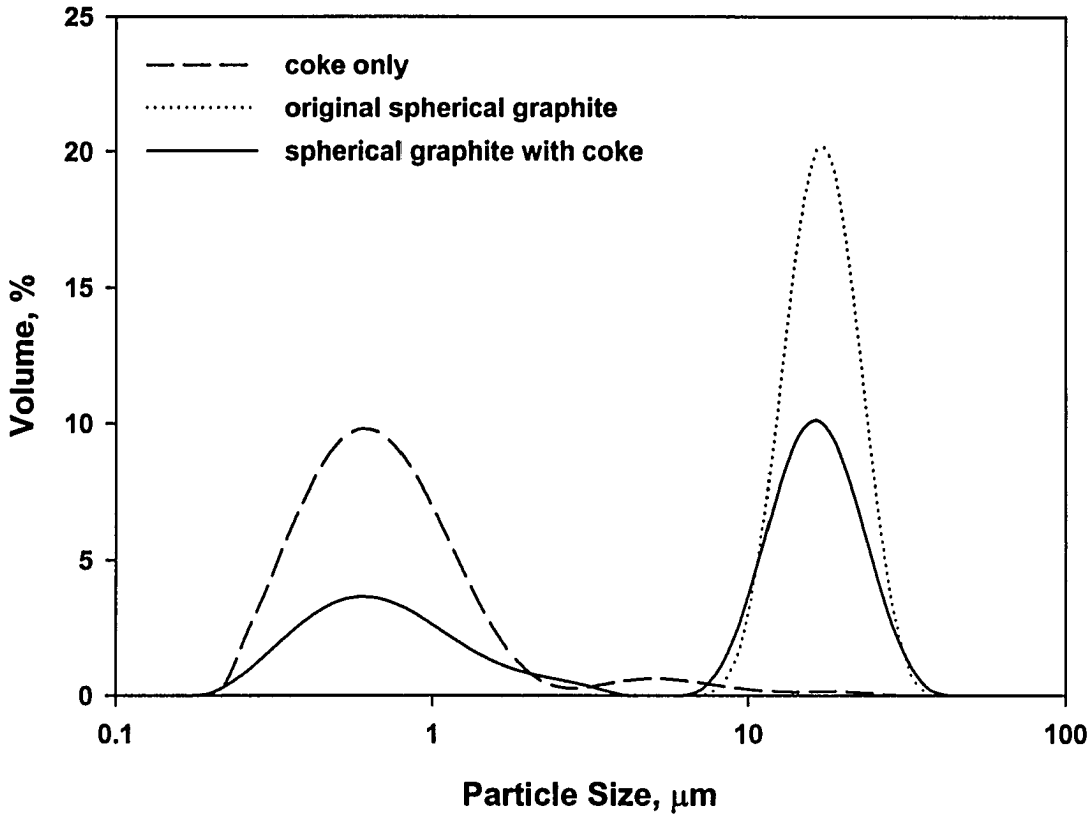

Figure 4.22 Effect of sonication on particle size distributions of TI products from 25 wt% AHVR in 1-MN without solid addition and with spherical graphite addition (0.06 g/g AHVR) at 430 °C and 40 min. TI products were suspended in ethanol and sonicated for 30 min.

wt% of total coke formed during the coking reaction deposited on the added spherical graphite particles. This estimation, however, was conservative because some coke deposits on the spherical graphite particles might be removed from the surface during sonication.

4.4.3 Dissolution of coke in tetralin

Under the standard coking conditions, the main reaction of TI products from coking reactions with tetralin would be hydrogen donation, expressed by the following formula, in which tetralin would convert into naphthalene by giving up its hydrogen while the coke would convert into toluene-soluble products:

$$\text{Tetralin } (C_{10}H_{12}) + \text{Coke} \rightarrow \text{Naphthalene}(C_{10}H_8) + \text{Toluene-soluble Products} \qquad (4\text{-}3)$$

Figure 4-23 (see repeated measurements in Table A4-2) shows the absorbances of diluted liquid products from reactions of the two TI products with tetralin under the standard coking conditions. Measurements at different wavelengths gave the same trend. The absorbance of the diluted liquid product from was much larger than from the reaction of coke-only material with tetralin, with the former being about 1.5 times of the latter.

The Beer-Lambert law is the linear relationship between absorbance and concentration of an absorbing species. Based on Beer-Lambert law and the calibration curve for absorbance of AHVR in tetralin (Figure A4-1), the concentration of the liquid product from the reaction of spherical graphite with coke material with tetralin was equivalent to 18.3 mg · AHVR/ml · tetralin, while 11.8 mg · AHVR/ml · tetralin for the liquid product from the reaction of coke-only material with tetralin. The larger the

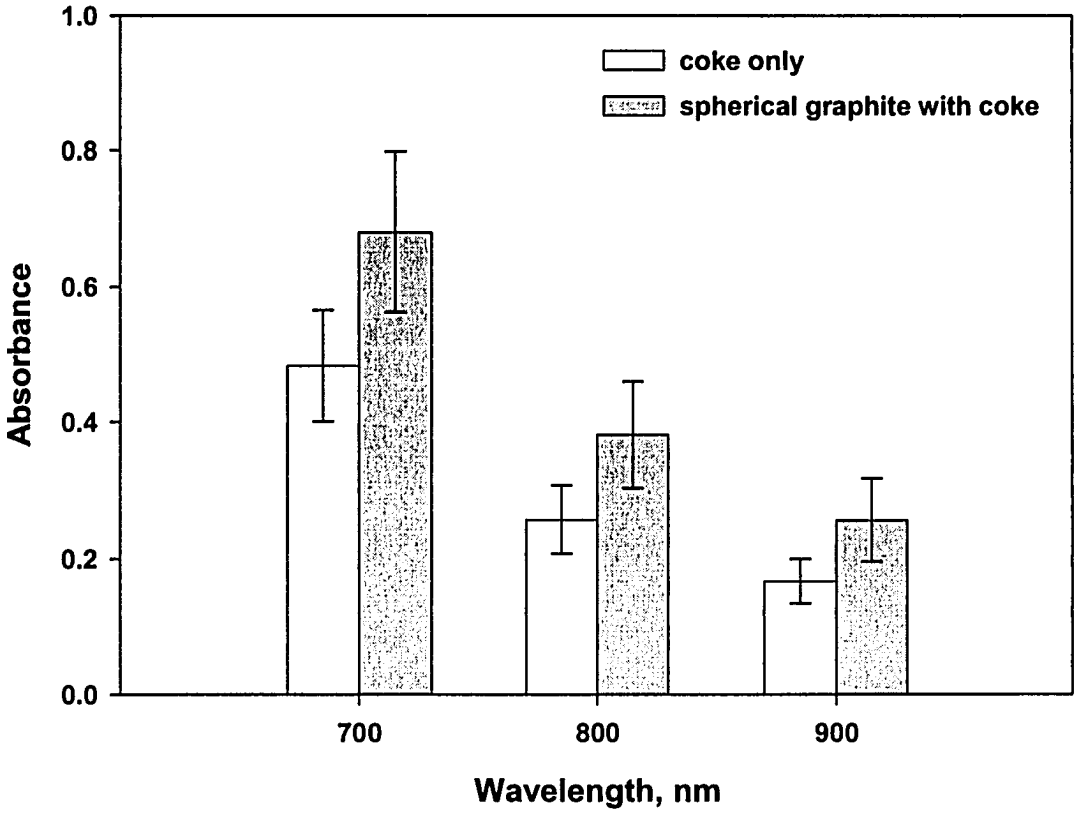

Figure 4.23 Absorbance of diluted liquid products (1 ml filtrate in 9 ml tetralin) from reactions of different TI solids (coke-only and spherical graphite with coke) with tetralin at 430 °C and 40 min.

concentration in tetralin, as determined by absorbance, the more coke was converted into toluene-soluble products. A contrast between the results of the two TI products with tetralin reactions was that although less coke was formed in the coking reaction with the presence of spherical graphite particles compared with the case without solid addition, more of this coke was converted into toluene-soluble products in the reaction with tetralin. This result suggested that compared with the coke-only particles, the particles of spherical graphite with coke were more accessible to the hydrogen donor in the reaction. This experiment also confirmed the role of hydrogen-transfer reactions between the coke phase and the bulk oil phase suggested by several other investigators (Gray, et al., 2001; Dutta, et al., 2001). Therefore, the second hypothesis proposed on the mechanism of lower coke yield due to solids was verified.

The more highly dispersed coke on the carbonaceous solids was more accessible to reactions with hydrogen donors. This mechanism is sufficient to explain the lower coke yields in figure 4-1, where the hydrogen donor reactions would be between the coke and the liquid-phase compounds of AHVR and their intermediate products due to cracking.

4.4.4 Other Roles of Fine Solids

Previous studies (Tanabe and Gray, 1997; Sanaie et al., 2001; Liu, 2002; Méndez et al., 2004) proved the ability of hydrophobic fine solids to retard coke formation during thermal cracking. Using the mesophase carbon and spherical graphite as additives in the coking reactions, this study further confirmed this role. Evidence in this work suggested the presence of fine solids could help disperse the new coke phase from coalescence during coking and made it more accessible to the hydrogen donor in the bulk oil phase,

leading to the reduced coke yield. Some other roles of fine solids in this process derived from observations in this work or proposed by some other investigators are discussed in the following sections.

(1) Emulsion Stabilizers

Tanabe and Gray (1997) proposed a hypothesis that the fine solids accumulated on the interface of a new phase of coke precursor and thereby stabilized the coke precursors from coalescence, analogous to the stabilization of oil-in-water emulsions and water-in-oil emulsions (Figure 2-7). The role of fine solids as emulsion stabilizers, however, was not applicable in this work because the coke precursors were much smaller than the added fine solids in length scale. Direct evidence from observations on the morphology of TI particles discussed earlier in this chapter also disclosed that the new coke phase that appeared during thermal cracking tended to wet the hydrophobic solid surface and form a thin layer of coke deposition but not in the reverse direction. Consequently, the role of fine particles was not analogous to solids in stabilizing emulsions.

(2) Free Radical Scavengers

Fine solids could inhibit the chain reactions of free radicals by providing more surface area for termination of radicals. Any significant suppression of free radical reaction due to the presence of solids would necessarily suppress the formation of gases, since gas formation was also mainly produced by free radical chain reactions (Tanabe and Gray, 1997). The possibility of bitumen solids as free radical scavengers was ruled out by previous studies (Tanabe and Gray, 1997; Liu, 2002), because the gas yields were

found to be almost unchanged within the reaction times, whether bitumen solids were present or not. In addition, the specific surface areas of mesophase carbon and spherical graphite materials used in the coking reactions were only 0.46 and 0.37 m^2/g, respectively. Therefore, the fine solids were unlikely to be significant as free radical scavengers.

(3) Catalytic Activities

Bitumen solids had mild catalytic activities towards hydrogenation, dehydrogenation and hydrogen shuttling that could be attributed to the presence of metallic elements such as iron, but their catalytic activity towards acidic cracking was insignificant (Liu, 2002). Compared with bitumen solids, the composition of mesophase carbon material used in this work was much simpler. Besides the main element of carbon, only several non-metallic elements such as hydrogen, oxygen, and nitrogen were present at low concentration (see Table 3-2). The other additive, spherical graphite material, was almost pure carbon in composition without any detectable trace elements. Therefore, it was very unlikely that fine solids employed in this work would display catalytic activities to cause reduced coke yields.

(4) Nucleation Sites

Hydrophobic solids could act as nucleation sites for phase separation during coke formation because the liquid coke phase was able to wet and spread on their surfaces. Although this mechanism had been stated by several investigators (Wang et al., 1998; Liu, 2002; Méndez et al., 2003), supporting evidence was quite absent. In this work, the

morphologies of TI particles from the coking reactions by SEM and EDX provided significant evidence of the fine solids acting as nucleation sites. The evidence also indicated that the submicron coke spheres spread on the solid surfaces, and would experience further coalescence and fusion to form a thin coke layer. The role of fine solids as nucleation sites directly resulted in a better-dispersed coke phase in the oil phase, as proven by the particle size distributions (Figure 4-20). The highly dispersed coke would have more contact with hydrogen donor compounds in the oil phase, which would in turn inhibit the rate of dehydrogenation and polymerization (Tanabe and Gray, 1997). In this work, the reactions of the TI products from coking reactions with tetralin suggest that the better-dispersed coke phase due to solids is more accessible to the hydrogen donors in the bulk liquid phase, leading to reduced coke yields. Therefore, based on all the evidence obtained in this work, the most likely role of fine solids in thermal cracking is to act as highly dispersed nucleation sites for coke deposition.

4.5 PROCESS IMPLICATIONS

1) The effect of hydrophobic fine solids on coke formation is relevant to a variety of feedstocks and fine solids. Bitumen solids separated from Athabasca bitumen display a significant impact on the initial kinetics of coke formation for Athabasca bitumen, its vacuum residue and Cold Lake bitumen. Some added fine solids, such as carbon black and asphaltene-treated kaolin, are also reported to be effective in coking of Athabasca bitumen and its vacuum residue. The mesophase carbon and spherical graphite used in this work also show a similar effect on the coking of AHVR, a naturally solids-free feedstock. Given the variety of fine solids and feedstocks used in coking reactions, the

role of hydrophobic fine solids to retard initial coke formation can be regarded as a general observation.

2) The understanding of coke deposition on fine solid surfaces could help us control fouling. Fouling problems are often attributed to coke formation under certain conditions. The experiments conducted in this work have confirmed that the new coke phase under moderate coking conditions deposits on the surfaces of added solids. Therefore, the presence of hydrophobic fine solids may help prevent or reduce deposition of coke material on the wall of furnace tubes and heat exchangers during delayed coking or visbreaking operations, which in turn would prolong the run length of units. When hydrophobic fine solids participate in thermal cracking, coke material will spread on the surfaces of fine solids, reducing the opportunity of coke deposition on the walls of process equipment.

5. CONCLUSIONS AND RECOMMENDATIONS

5.1 CONCLUSIONS

5.1.1 Fine Solids on Coke Formation

In this work, the effect of fine solids on coke formation was investigated under a moderate severity of coking conditions at a fixed, short reaction time. Two powdered solids, mesophase carbon and spherical carbon, were employed as additives during coking of AHVR in 1-MN. A pronounced drop in coke yield, 23 wt% for the mesophase carbon and 32 wt% for the spherical graphite, was obtained compared with the case where no fine solid was added. The ability of hydrophobic fine solids in retarding the initial kinetics of coke formation, therefore, was further confirmed.

5.1.2 Interaction between Coke and Fine Solids

The morphologies of TI particles from coking of AHVR in 1-MN, with or without solid addition, were studied by SEM. The comparison on micrographs of both the whole particles and their cross sections suggested that the new coke phase that formed during coking tended to wet and spread on the surfaces of added solids to form a thin coke film. Based on the distinct composition difference between the coke material and the carbonaceous particles in sulfur content, the interaction between coke and model solids was confirmed by EDX analysis. All information from the morphology study confirmed that the carbonaceous solids acted either as nucleation sites for the coke phase formed during coking of AHVR in 1-MN, or a compatible surface for agglomeration of coke phase after it formed.

5.1.3 Pathway of Coke Deposition on Solids

The pathway of coke deposition on fine solids was investigated by changing the ratio of AHVR to added solids in the coking reactions. Evidence from SEM, EDX and XPS analyses indicated that the pathway of coke deposition depended on the ratio of AHVR to surface area of the fine solids. At very low ratios of AHVR to fine solids, the coke deposited directly on the surface of the fine solids in nanometer-scale layers. As the ratio of AHVR to fine solids increased, the coke phase appeared to form first in the liquid phase as submicron scale spheres, which then deposited on the fine solids. These surface deposits of submicron material subsequently underwent further coalescence and fusion.

5.1.4 Mechanism of Reduced Coke Yield due to Solids

Hydrophobic fine solids could disperse the new coke phase formed during coking reactions. This hypothesis was supported by the particle size distribution data in this work. As suggested by the results from reactions of TI products with tetralin, the highly dispersed coke was more accessible to hydrogen donor compounds in the oil phase, which in turn inhibited the initial rate of coke formation. The basis of this mechanism, however, was the role of fine solids as nucleation sites for coke deposition during thermal cracking.

5.2 RECOMMENDATIONS

1) The temperature at which the coking reactions were done in this work was comparatively lower than the real temperatures that are being employed in industrial coking furnaces. In addition, previous studies suggested that the effect of hydrophobic fine solids on coke formation was pronounced at short reaction times but became unremarkable at prolonged reaction times, which raised the question whether or not hydrophobic fine solids could reduce the ultimate coke yield in commercial units. Therefore, repetition of these experiments under an increased severity of coking conditions (both temperature and time) would generate more practical data for potential industrial applications.

2) The use of fine solids as additives to control fouling may be an interesting direction for future work towards commercial applications. In order to select the most effective additive, all aspects of fine solids in oil suspension such as concentration, particle size, wettability, coalescence and hydrodynamics should be taken into account.

3) In this work, the interaction between the coke phase and the added solids was determined by studying the TI particles. The influence of the quenching process and TI separation process on the interaction between the coke and added solids, however, is not clear. Similar uncertainty is also involved in the particle size distribution measurement. A device that works "in situ", such as hot-stage microscopy, might be able to provide valuable information on the real situation in the reactor by monitoring the development of the coke phase, its deposition on the surfaces of fine solids, etc.

REFERENCES

Alboudwarej H.; Beck J.; Svrcek W. Y.; Yarranton H. W. Sensitivity of Asphaltene Properties to Separation Techniques. *Energy Fuels* **2002**, 16, 462-469.

Asprino O. J.; Elliott J. A. W.; McCaffrey W. C.; Gray M. R. Fluid Properties of Asphaltenes at 310-530 °C. *Energy Fuels* **2005** (web release date: May 18, 2005).

Attalla, M. I.; Bruce, L. A.; Hodgson, S. I.; Turney, T. W.; Wilson, M. A.; Batts, B. D. Reactions of coal liquids with cross-linked smectite catalysts 1. Effects of pillaring materials and recycling. *Fuel* **1990**, 69, 725-734.

Banerjee, D. K., Laidler, K. J., Nandi, B. N., Patmore, D. J. Kinetic Studies of coke formation in hydrocarbon fractions of heavy crudes. *Fuel* **1986**, 65, 480-484.

Bardon, C.; Barre L.; Espinat, D.; Guille, V.; Li, M. H.; Lambard, J.; Ravey, J. C.; Rosenberg, E.; Zemb, T. The Colloidal Structure of Crude Oils and Suspensions of Asphaltenes and Resins. *Fuel Sci. Tech. Int.* **1996**, 14(1&2), 203-242.

Bensebaa, F.; Kotlyar, L. S.; Sparks, B. D.; Chung, K. H. Organic Coated Solids in Athabasca Bitumen: Characterization and Process Implications. *Can. J. Chem. Eng.* **2000**, 78, 610-616.

Breen, C.; Zahoor, F. D.; Madejová J.; Komadel, P. Characterization and Catalytic Activity of Acid-Treated, Size-Fractionated Smectites. *J. Phys. Chem. B* **1997**, 101, 5324-5331.

Brooks, J. D., Taylor, G. H. Formation of Graphitizing Carbons from the Liquid Phase. *Nature* **1965**, 206, 697-699.

Brooks, J. D.; Taylor, G. H. The Formation of Some Graphitizing Carbons. *Chemistry and Physics of Carbon* (P. L. Walker Jr., Editor) **1968**, 4, 243-286.

Butt, J. B.; Petersen, E. E. *Activation, Deactivation, and Poisoning of Catalysts.* Academic Press, San Diego. **1988.**

Champagne, P. J.; Manolakis, E.; Ternan, M. Molecular weight distribution of Athabasca bitumen. *Fuel* **1985**, 64, 423-425.

Chung, K. H.; Xu, S.; Gray, M. R.; Zhao, Y.; Kotlyar, L. S.; Sparks, B. D. The chemistry, reactivity and processability of Athabasca bitumen pitch. *Rev. Process Chem. Eng.* **1998**, 1, 41-79.

Dickie, J. P.; Yen, T. F. Macrostructures of the Asphaltic Fractions by Various Instrumental Methods. *Anal. Chem.* **1967**, 39, 1847-1852.

Dutta, R. P.; McCaffrey, W. C.; Gray, M. R. Use of ^{13}C Tracers to Determine Mass-Transfer Limitations on Thermal Cracking of Thin Films of Bitumen. *Energy Fuels* **2001**, 15, 1087-1093.

Fouda, S. A.; Kelly, J. F.; Rahimi, P. M. Effects of Coal Concentration on Coprocessing Performance. *Energy Fuels* **1989**, 3, 154-160.

Fukuda, N.; Nagayama, K.; Honma, M. Manufacturing Processes and Characteristics of KMFC Powder and KMFC Graphite Blocks. *Kawasaki Steel Technical Report*, No. 23, October **1990.**

Gentzis T.; Rahimi P.; Malhotra R.; Hirschon, A. S. The effect of carbon additives on the mesophase induction period of Athabasca bitumen. *Fuel Process. Tech.* **2001**, 69, 191-203.

Gray, G. W.; Winsor, P. A. *Liquid Crystals and Plastic Crystals.* Ellis Horwood Ltd., Chichester. **1973.**

Gray, M. R. *Upgrading Petroleum Residues and Heavy Oils.* Marcel Dekker, Inc., New York. **1994.**

Gray, M. R.; Le, T.; McCaffrey, W. C.; Berruti, F.; Soundararajan, S.; Chan, E.; Huq I.; Thorne, C. Coupling of Mass Transfer and Reaction in Coking of Thin Films of an Athabasca Vacuum Residue. *Ind. Eng. Chem. Res.* **2001**, 40, 3317-3324.

Gray, M. R.; McCaffrey, W. C.; Huq I.; Le T. Kinetics of Cracking and Devolatilization during Coking of Athabasca Residues. *Ind. Eng. Chem. Res.* **2004**, 43, 5438-5445.

Groenzin H.; Mullins, O. C. Molecular Size and Structure of Asphaltenes from Various Sources. *Energy Fuels* **2000**, 14, 677-684

Herzog, P.; Tchoubar, D.; Espinat, D. Macrostructure of asphaltene dispersions by small-angle X-ray scattering. *Fuel* **1988**, 67, 245-250.

Jewell, D. M.; Albaugh, E. W.; Davis, B. E.; Ruberto, R. G. Integration of Chromatographic and Spectroscopic Techniques for the Characterization of Residual Oils. *Ind. Eng. Chem. Fundam.* **1974**, 13(3), 278-282.

Kapustin S. M.; Stolonogov, I. I.; Zaitseva, N. P.; Syunyaev, Z. I. Coalescence of Particles of Liquid Crystal Phase in Coking Residual Petroleum Stocks. *Chem. Technol. Fuels Oils* **1983**, 19 (3&4), 204-206.

Koots, J. A.; Speight, J. G. Relation of petroleum resins to asphaltenes. *Fuel* **1975**, 54, 179-184.

Korai, Y.; Wang, Y-G.; Yoon, S-H.; Ishida, S.; Mochida, I.; Nakagawa Y.; Matsumura, Y. Preparation of meso-carbon microbeads with uniform diameter from AR-isotropic pitch in the presence of carbon black. *Carbon* **1996**, 34 (9), 1156-1159.

Kotlyar, L. S.; Sparks, B. D. Properties of Fines Size Fraction in Relation to the Distribution of Humic-Inorganic Matter Complexes in Athabasca Oil Sands. *AOSTRA J. Res.* **1988**, 4, 277-285.

Kotlyar, L. S.; Sparks, B. D.; Woods, J. R., Raymond, S., Le Page, Y.; Shelfantook, W. Distribution and Types of Solids Associated with Bitumen. *Petrol. Sci. Tech.* **1998**, 16, 1-19.

Kumagai, H. Kinetic study on dissociation of asphaltene aggregates by means of proton NMR relaxation measurements. Presented at *The 4th International Conference on petroleum Phase Behavior and Fouling*, June 23-26, **2003**, Norway.

LaMarca, C.; Libanati, C.; Klein M. T. Enhancing Chain Transfer during Coal Liquefaction: A Model System Analysis. *Energy Fuels* **1993**, 7, 473-478.

Lemke, H. K.; Stephenson, W. K. Deposit Formation in Industrial Delayed Coker / Visbreaker Heaters. *Petrol. Sci. Tech.* **1998**, 16 (3&4), 335-360.

Li, S.; Liu, C.; Que, G.; Liang W. Colloidal structures of vacuum residua and their thermal stability in terms of saturate, aromatic, resin and asphaltene composition. *J. Petrol. Sci. Eng.* **1999**, 22, 37-45.

Lian, H. J.; Lee, C.; Yen, T. F. Fractionation of Asphalt by Thin-Layer Chromatography Interfaced with Flame Ionization Detector (TLC-FID) and Subsequent Characterization by FTIR. *Asphaltene Particles in Fossil Fuel Exploration, Recovery, Refining, and Production Processes.* M. K. Sharma and T. F. Yen (Eds.), Plenum Press, New York. **1994.**

Liu, L. Effect of Solids on Coke Formation from Athabasca Bitumen and Vacuum Residue. *Ph.D. Thesis - University of Alberta* **2002**.

Loeber, L.; Muller, G.; Morel J.; Sutton, O. Bitumen in colloid science: a chemical, structural and rheological approach. *Fuel* **1998**, 77, 1443-1450.

Magaril, R. Z.; Aksenova, E. I. Study of the Mechanism of Coke Formation in the Cracking of Petroleum Resins. *Int. Chem. Eng.* **1968**, 8, 727-729.

Magaril, R. Z.; Ramazeava, L. F.; Aksenova, E. I. Kinetics of the Formation of Coke in Thermal Processing of Crude Oil. *Int. Chem. Eng.* **1971**, 11, 250-251.

McMillen, D. F.; Golden, D. M. Hydrocarbon Bond Dissociation Energy. *Annu. Rev. Phys. Chem.* **1982**, 33, 493-532.

Méndez, A.; Santamaría, R.; Granda, M.; Menéndez, R. Influence of Granular Carbons on he Thermal Reactivity of Pitches. *Energy Fuels* **2004**, 18, 22-29.

Mochida, I.; Oyama, T.; Korai, Y.; Fei, Y. Study of carbonization using a tube bomb: evaluation of lump needle coke, carbonization mechanism and optimization. *Fuel* **1988**, 67, 1171-1181.

Moschopedis, S. E.; Fryer, J. F.; Speight, J. G. Investigation of asphaltene molecular weights. *Fuel* **1976**, 55, 227-232.

Murgich J.; Abanero J. A.; Strausz O. P. Molecular Recognition in Aggregates Formed by Asphaltene and Resin Molecules from the Athabasca Oil Sand. *Energy Fuels* **1999**, 13, 278-286.

Nandi, B. N.; Pruden, B. B; Parsons, B. I.; Montgomery, D. S. Microscopic changes in the coal-based catalyst used in the hydrocracking of Athabasca bitumens. *Fuel* **1978**, 57, 722-726.

Petroleum Communication Foundation, *Canada's Oil Sands and Heavy Oil.* Calgary, Alberta. **2000.**

Pfeiffer J. Ph.; Saal R. N. J. Asphaltic Bitumen as a Colloid System. *J. Phys. Chem.* **1940**, 44, 139-149.

Poutmas, M. L. Free-Radical Thermolysis and Hydrogenolysis of Model Hydrocarbons Relevant to Processing of Coal. *Energy Fuels* **1990**, 4(2), 113-131.

Poutmas M. L. Fundamental reactions of free radicals relevant to pyrolysis reactions. *J. Anal. Appl. Pyrolysis* **2000**, 54, 5-35.

Rahimi P.; Gentzis T.; Dawson, W. H.; Fairbridge, C.; Khulbe, C.; Chung, K.; Nowlan, V.; DelBianco A. Investigation of Coking Propensity of Narrow Cut Fractions from Athabasca Bitumen Using Hot-Stage Microscopy. *Energy Fuels* **1998**, 12, 1020-1030.

Rahimi, P.; Gentzis T.; Fairbridge, C. Interaction of Clay Additives with Mesophase Formed during Thermal Treatment of Solid-Free Athabasca Bitumen Fraction. *Energy Fuels* **1999**, 13, 817-825.

Rahmani S.; McCaffrey W.; Elliott, J. A. W.; Gray, M. R. Liquid-Phase Behavior during the Cracking of Asphaltenes. *Ind. Eng. Chem. Res.* **2003**, 42, 4101-4108.

Rice, F. O.; Herzfeld, K. F. The Thermal Decomposition of Organic Compounds from the Standpoint of Free Radicals. VI. The mechanism of Some Chain Reactions. *J. Am. Chem. Soc.* **1934**, 56, 284-289.

Rosa-Brussin, M. The Use of Clays for the Hydrotreatment of Heavy Crude Oils. *Catal. Rev. Sci. Eng.* **1995**, 37(1), 1-100.

Sanaie, N.; Watkinson, A. P.; Bowen, B. D.; Smith, K. J. Effect of minerals on coke precursor formation. *Fuel* **2001**, 80, 1111-1119.

Sanford, E. C. The Nomenclature and Jargon of Residuum Upgrading: A Critical Review. *AOSTRA J. Res.* **1991**, 7, 201-208.

Schucker, P. C.; Keweshan, C. F. The Reactivity of Cold Lake Asphaltenes. *Preprints, Div. Fuel Chem. Am. Chem. Soc.*, **1980**, 25, 155-165.

Savage, P. E.; Klein, M. T.; Kukes, S. G. Asphaltene Reaction Pathways. 1. Thermolysis. *Ind. Eng. Chem. Proc. Des. Dev.* **1985**, 24, 1169-1174.

Savage, P. E.; Klein, M. T. Asphaltene Reaction Pathways. 3. Effect of Reaction Environment. *Energy Fuels* **1988**, 2, 619-628.

Savage, P. E. Mechanisms and Kinetics models for Hydrocarbon Pyrolysis. *J. Anal. Appl. Pyrolysis* **2000**, 54, 109-126.

Sheremata, J. M.; Gray, M. R.; Dettman, H. D.; McCaffrey, W. C. Quantitative Molecular Representation and Sequential Optimization of Athabasca Asphaltenes. *Energy Fuels* **2004**, 18, 1377-1384.

Sparks, B. D.; Kotlyar, L. S.; O'Carroll J. B.; Chung, K. H. Athabasca oil sands: effect of organic coated solids on bitumen recovery and quality. *J. Petrol. Sci. Eng.* **2003**, 39, 417-430.

Speight J. G.; Wernick, D. L.; Gould, K. A.; Overfield, R. E.; Rao, B. M. L.; Savage, D. W. Molecular Weight and Association of Asphaltenes: A Critical Review. *Rev. Inst. Franc. Petrol.* **1985**, 40(1), 51-61.

Speight, J. G. *The Chemistry and Technology of Petroleum*. 2nd edition, Marcel Dekker, Inc., New York, **1991**.

Speight, J. G. Asphaltenes and Asphalts, 1. Yen, T. F. and Chilingarian, G. V., Eds., Elsevier Science, New York, **1994**, Chapter 2.

Speight, J. G.; Long, R.B. The Concept of Asphaltenes Revisited. *Fuel Sci. Tech. Int.* **1996**, 14(1&2), 1-12.

Speight, J. G.; Özüm, B. *Petroleum Refining Processes*. Marcel Dekker, Inc., New York. **2002**.

Srinivasan N. S.; McKnight, C. A. Mechanism of coke formation from hydrocracked Athabasca residuum. *Fuel* **1994**, 73, 1511.

Storm, D. A.; Barresi, R. J.; DeCanio, S. J. Colloidal nature of vacuum residue. *Fuel* **1991**, 70, 779-782.

Storm, D. A.; Edwards, J. C.; DeCanio, S. J.; Sheu, E. Y. Molecular Representations of Ratawi and Alaska North Slope Asphaltenes Based on Liquid- and Solid-State NMR. *Energy Fuels* **1994**, 8, 561-566.

Storm, D. A.; Barresi, R. J.; Sheu, E. Y. Flocculation of Asphaltenes in Heavy Oil at Elevated Temperatures. *Fuel Sci. Tech. Int.* **1996**, 14(1&2), 243-260.

Strausz, O. P.; Mojelsky, T. W.; Lown, E. M. The molecular structure of asphaltene: an unfolding story. *Fuel* **1992**, 71, 1355-1363.

Strausz, O. P.; Peng, P.; Murgich J. About the Colloidal Nature of Asphaltenes and the MW of Covalent Monomeric Unites. *Energy Fuels* **2002**, 16, 809-822.

Strausz, O. P.; Lown, E. M., *The Chemistry of Alberta Oil Sands, Bitumens and Heavy*

Oils **2003**, Alberta Energy Research Institute, Calgary, Alberta, Canada.

Tanabe, K.; Gray, M. R. Role of Fine Solids in the Coking of Vacuum Residues. *Energy Fuels* **1997**, 11, 1040-1043.

Tanaka, R.; Sato, E.; Hunt, J. E.; Winans, R. E.; Sato S.; Takanohashi T. Characterization of Asphaltene Aggregates Using X-ray Diffraction and Small-Angle X-ray Scattering. *Energy Fuels* **2004**, 18, 1118-1125.

Wang, S.; Chung, K.; Masliyah, J. H.; Gray, M. R. Toluene-insoluble fraction from thermal cracking of Athabasca gas oil: formation of a liquid-in-oil emulsion that wets hydrophobic dispersed solids. *Fuel* **1998**, 77, 1647-1653.

Watkinson, A. P.; Wilson, D. I. Chemical Reaction Fouling – A Review. *Exp. Therm. Fluid Sci.* **1997**, 14, 361-374.

Wiehe, I. A. A Solvent-Resid Phase Diagram for Tracking Resid Conversion. *Ind. Eng. Chem. Res.* **1992**, 31, 530-536.

Wiehe, I. A. A Phase-Separation Kinetic Model for Coke Formation. *Ind. Eng. Chem. Res.* **1993**, 32, 2447-2454.

Wiehe, I. A.; Liang, K. S. Asphaltenes, Resins and other Petroleum Macromolecules. *Fluid Phase Equilib.* **1996**, 117, 201-210.

Wolk, R. H. Hydroconversion of Tar Sand Bitumens. *US Patent 3,844,937*; **1974**.

Zander, M. On the Composition of Pitches. *Fuel* **1987**, 66, 1536-1539.

APPENDICES

A. EXPERIMENTAL DATA

A1 Coke Yields

Table A1-1 Coke yields from coking without and with fine solid addition

Feed (g)			Run #	Coke Yield	Avg. of coke	Standard
AHVR	1-MN	Additive		(wt%)	yield (wt%)	deviation
1.5	4.5	None	1	8.57	9.29	±0.84
			2	10.50		
			3	9.08		
			4	9.00		
1.5	4.5	0.09 (mesophase carbon)	1	6.65	7.15	±0.86
			2	8.15		
			3	6.66		
1.5	4.5	0.09 (spherical graphite)	1	6.37	6.29	±0.23
			2	6.46		
			3	6.03		

A2 Sulfur Content of Coke

Table A2-1 Sulfur content of coke from coking without fine solid addition

Coke sample	Run #1	Run #2	Run #3
Mass of sample (mg)	1.5	1.5	1.4
Scnts/Wt	21649	25631	19863
Mass of sulfur (mg)	0.103	0.119	0.096
Sulfur content (wt%)	6.87	7.93	6.86
Average of Sulfur content (wt%)		7.22	
Standard deviation		±0.61	

Sulfur calibration for coke used:

Mass of sulfur (mg) = 4E-06 * Scnts/Wt + 0.0161

A3 Particle Size Distributions

Table A3-1 Particle size distributions of fine solid additives- thermal stability check

Size (μm)	Mesophase carbon[a] (vol%)	Mesophase carbon[b] (vol%)	Spherical graphite[a] (vol%)	Spherical graphite[b] (vol%)
0.83		0.00		
0.96	0.00	0.02		
1.10	0.02	0.08		
1.26	0.11	0.11		
1.45	0.14	0.14		
1.66	0.18	0.18		
1.91	0.22	0.22		
2.19	0.27	0.28		
2.51	0.35	0.36		
2.88	0.47	0.47		
3.31	0.65	0.64		
3.80	0.91	0.89		
4.37	1.26	1.22		
5.01	1.73	1.67		
5.75	2.33	2.25	0.00	0.00
6.61	3.06	2.97	0.01	0.01
7.59	3.92	3.82	0.32	0.31
8.71	4.86	4.76	1.73	1.68
10.00	5.86	5.77	5.21	5.12
11.48	6.80	6.74	10.68	10.58
13.18	7.64	7.62	16.59	16.55
15.14	8.26	8.29	19.99	20.03
17.38	8.59	8.66	19.01	19.12
19.95	8.55	8.66	14.20	14.31
22.91	8.12	8.24	8.08	8.13
26.30	7.32	7.43	3.35	3.35
30.20	6.21	6.30	0.78	0.76
34.67	4.93	4.99	0.04	0.04
39.81	3.60	3.65	0.00	0.00
45.71	2.38	2.39		
52.48	1.19	1.15		
60.26	0.04	0.04		
69.18	0.00	0.00		
79.43				

[a] Original size distributions of the fine solid additives.

[b] Size distributions of the fine solid additives after thermal stability check.

Table A3-2 Comparison of particle size distributions for coke only and SG with coke (Solid samples were suspended in ethanol and shaken for 1 minute)

Size (μm)	Coke only (vol%)	Spherical graphite with coke (vol%)	Size (μm)	Coke only (vol%)	Spherical graphite with coke (vol%)
0.182	0.00		11.482	1.76	3.51
0.209	0.02	0.00	13.183	1.74	4.03
0.240	0.14	0.03	15.136	1.72	4.34
0.275	0.58	0.34	17.378	1.69	4.38
0.316	0.99	0.65	19.953	1.65	4.12
0.363	1.46	1.01	22.909	1.62	3.62
0.417	1.91	1.37	26.303	1.58	2.95
0.479	2.30	1.71	30.200	1.54	2.23
0.550	2.63	2.02	34.674	1.50	1.56
0.631	2.85	2.27	39.811	1.47	1.03
0.724	2.96	2.46	45.709	1.45	0.68
0.832	2.96	2.60	52.481	1.45	0.50
0.955	2.88	2.68	60.256	1.47	0.48
1.096	2.72	2.73	69.183	1.51	0.58
1.259	2.51	2.76	79.433	1.58	0.76
1.445	2.29	2.76	91.201	1.69	0.98
1.660	2.07	2.76	104.713	1.84	1.18
1.905	1.89	2.75	120.226	2.03	1.33
2.188	1.76	2.71	138.038	2.25	1.36
2.512	1.69	2.64	158.489	2.46	1.26
2.884	1.66	2.51	181.970	2.60	1.00
3.311	1.68	2.32	208.930	2.61	0.63
3.802	1.71	2.09	239.883	2.39	0.38
4.365	1.75	1.84	275.423	1.92	0.19
5.012	1.77	1.63	316.228	1.30	0.02
5.754	1.78	1.53	363.078	0.81	0.00
6.607	1.78	1.60	416.869	0.23	
7.586	1.78	1.86	478.630	0.04	
8.710	1.78	2.32	549.541	0.00	
10.000	1.77	2.91	630.957		
11.482					

Table A3-3 Particle size distributions of solid products from coking after sonication (Solid products were suspended in ethanol and sonicated for 30 minutes)

Size (μm)	Coke only (vol%)	Spherical graphite with coke (vol%)	Size (μm)	Coke only (vol%)	Spherical graphite with coke (vol%)
0.158	0.00	0.00	2.884	0.30	0.37
0.182	0.05	0.05	3.311	0.42	0.18
0.209	0.50	0.37	3.802	0.54	0.02
0.240	2.16	0.85	4.365	0.61	0.00
0.275	3.71	1.45	5.012	0.62	0.00
0.316	5.47	2.09	5.754	0.56	0.00
0.363	7.07	2.69	6.607	0.47	0.20
0.417	8.43	3.18	7.586	0.36	1.02
0.479	9.36	3.51	8.710	0.27	2.62
0.550	9.79	3.65	10.000	0.19	4.97
0.631	9.68	3.59	11.482	0.15	7.48
0.724	9.07	3.36	13.183	0.13	9.45
0.832	8.05	2.99	15.136	0.14	10.13
0.955	6.73	2.54	17.378	0.15	9.30
1.096	5.29	2.08	19.953	0.12	7.30
1.259	3.85	1.65	22.909	0.08	4.81
1.445	2.57	1.29	26.303	0.02	2.58
1.660	1.55	1.01	30.200	0.00	1.03
1.905	0.83	0.81	34.674		0.20
2.188	0.42	0.66	39.811		0.00
2.512	0.27	0.52	45.709		
2.884					

A4 Absorbances

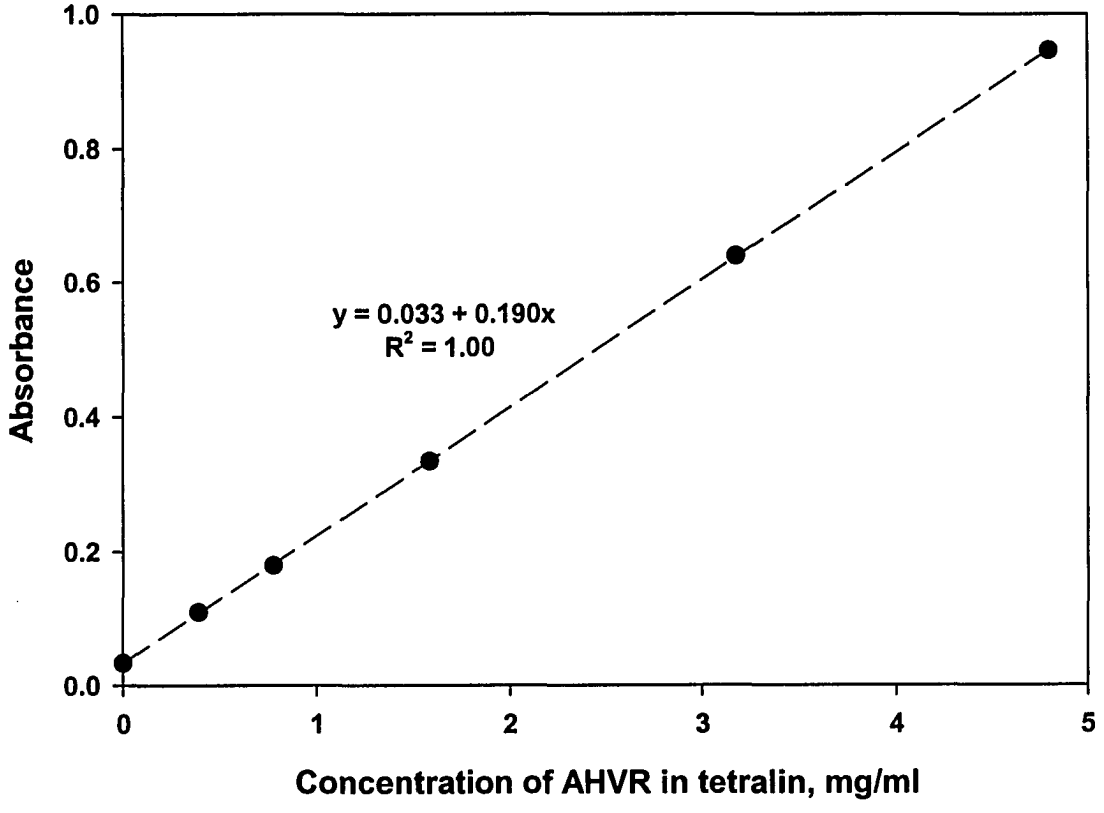

Figure A4-1 Calibration curve for absorbance of AHVR in tetralin

Table A4-1 Absorbances of standard solutions of AHVR dissolved in tetralin

Concentration (mg/ml)	0.39	0.78	1.58	3.18	4.80
Absorbance at 800nm	0.11	0.18	0.33	0.64	0.95

Table A4-2 Absorbances of diluted liquid products (1 ml filtrate in 9 ml tetralin) from reactions of different solids with tetralin

Index	Absorbance					
Wavelength	700 nm		800nm		900 nm	
Solid	Coke only	SG with coke	Coke only	SG with coke	Coke only	SG with coke
Run #1	0.392	0.631	0.204	0.341	0.132	0.218
Run #2	0.505	0.595	0.266	0.331	0.172	0.225
Run #3	0.552	0.815	0.302	0.472	0.197	0.326
Average	0.483	0.680	0.257	0.381	0.167	0.256
Standard deviation	± 0.082	± 0.118	± 0.050	± 0.079	± 0.033	± 0.060

B. MOUNTING AND POLISHING PROCEDURES

B1 Mounting Procedure

A JH-5 mounting press (ENERPAC, Butler, WI) was used to mold samples.

1. Make sure surfaces of mold assembly are clean and free of residue.
2. Spray all contacting Surfaces with "Silicone Mold Release".
3. Insert specimen (toluene-insoluble particles) and add molding material (lucite or green bakelite).
4. Stir specimen and molding material to make a uniform mixture.
5. Insert ram and put the mold in place.
6. Heat mold assembly to 65 °C under a pressure of 3000 psi.
7. Increase pressure to 6000 psi and continue heating until temperature reaches 140 °C (for green bakelite) or 150 °C (for lucite).
8. Turn off heat once the temperature reaches 140 °C or 150°C and release pressure (for green bakelite but not lucite).
9. Cool mold assembly to 80 °C (cool under pressure for lucite.).
10. Remove sample using pumping unit.

B2 Polishing Procedure

1. Polish one sample surface on an 80 grit abrasive belt.
2. Turn 90 degree of the surface and polish it on a 120 grit abrasive belt until the first scratch is removed.
3. Polish the surface on a series of METASERV 2000 grinders (BUEHLER, Lake Bluff, IL) in the sequence of 240, 320, 400 and 600 grit.
4. Continue to polish the surface on a series of METASERV 2000 grinders using 6-micron diamond paste, 1.0-micron magomet and 0.05-micron alumina.
5. Clean the sample to remove the entire residue from the surface.

C. CALCULATION OF MASS MOMENT MEAN RADIUS

Sample: spherical graphite with coke (Table A3-2)

The Mass moment mean radius (R_{43}) of the coke material in the TI sample is calculated as follows:

$$R_{43} = \frac{R'_{43} \times M_1 + T \times M_2}{M}$$

where

R_{43} is the mass moment mean radius of the coke material in the TI sample,

R'_{43} is the mass moment mean radius of the separate coke particles,

M is the total mass of coke material formed in the coking reaction,

M_1 is the mass of separate coke particles,

M_2 is the mass of coke deposits on the spherical graphite particles, and

T is the mean thickness of coke deposits on the spherical graphite surface.

(1) The total mass of coke material is calculated using the coke yield.

From Table A1-1: $M = 1.5 \times 0.0629 = 0.0943$ (g)

(2) Assume that the mass moment mean radius of separate coke particles in the TI sample is the same as that of the coke-only sample listed in Table A3-2.

From the Mastersizer data: $R'_{43} = 27.9$ μm

(3) Assume the mass of separate coke particles is the same as that of those in the spherical graphite with coke sample listed in Table A3-3.

From Table A3-3: The separate coke particles account for 38.91 vol% in the spherical graphite with coke sample.

Let $\rho^{a}_{coke} = 1.2$ g/cm^3, $\rho^{b}_{graphite} = 2.25$ g/cm^3

[a] Refer to the density of asphaltenes reported by Alboudwarej et al. (2002)

[b] Take as an average from true density range of graphite: 1.9-2.3 g/cm^3

Total volume of the spherical graphite with coke material:

$V = 0.0943/1.2 + 0.09/2.25 = 0.1186$ (cm^3)

The mass of separate coke particles: $M_1 = 0.1186 \times 0.3891 \times 1.2 = 0.0554$ (g)

(4) The mass of coke deposits on the spherical graphite particles is:

$M_2 = M - M_1 = 0.0943 - 0.0554 = 0.0389$ (g)

(5) Assume the mean thickness of coke deposits on the spherical graphite particles is the same as that of the spherical graphite with coke sample listed in Table A3-3.

The calculation of the mean thickness is based on the following assumptions:

(i) All the solid particles are perfect spheres.

(ii) All the solid particles are non-porous.

(iii) The thickness of coke deposits on the spherical graphite surface is uniform.

From to the Mastersizer data, the sauter mean diameter and the specific surface area of the original spherical graphite particles are:

$D_{32, graphite} = 16.30$ μm, $A_{graphite} = 0.369$ m^2/g

The surface area of the 0.09 g of added spherical graphite is:

$A = 0.09 \times 0.369 = 0.03321$ m^2

The number of particles with a sauter mean diameter in the 0.09 g of spherical graphite is:

$N = 0.03321 / [\pi \times (16.30 \times 10^{-6})^2] = 3.9787 \times 10^7$

The volume of coke deposits on the spherical graphite surface is:

$V_{coke\ on\ graphite} = 0.0943/1.2 - 0.1186 \times 0.3891 = 0.03244$ (cm^3)

The mean diameter of the particles of spherical graphite with coke deposits is:

$$V_{\text{coke on graphite}} = N \times \{4/3 \times \pi \times [(D_{\text{graphite with coke deposits}}/2)^3 - (D_{32,\text{ graphite}}/2)^3]\}$$

$$= 3.9787 \times 10^7 \times \{4/3 \times \pi \times [(D_{\text{graphite with coke deposits}}/2)^3 - (16.30/2)^3]\}$$

$$= 0.03244 \times 10^{12}$$

Then we get: $D_{\text{graphite with coke deposits}} = 18.06\ \mu m$

The mean thickness of coke deposits on the spherical graphite surface is:

$$T = [D_{\text{graphite with coke deposits}} - D_{32,\text{ graphite}}]/2 = (18.06 - 16.30)/2 = 0.88\ \mu m$$

Hence, the mass moment mean radius of the coke material in the TI sample is:

$$R_{43} = \frac{27.9 \times 0.0554 + 0.85 \times 0.0389}{0.0943} = 16.7 \mu m$$